bioRxiv preprint doi: https://doi.org/10.1101/2021.04.01.438020; this version posted May 24, 2021. The copyright holder for this preprint (which was not certified by peer review) is the author/funder. All rights reserved. No reuse allowed without permission.

Screening of HLA-A restricted T cell epitopes of SARS-CoV-2 and induction of $CD8^+$ T cell responses in HLA-A transgenic mice

Xiaoxiao Jin[1#], Yan Ding[1#], Shihui Sun[2#], Xinyi Wang[1], Zining Zhou[1], Xiaotao Liu[1], Miaomiao Li[3], Xian Chen[3], Anran Shen[4], Yandan Wu[1], Bicheng Liu[4], Jianqiong Zhang[1], Jian Li[5], Yi Yang[6], Haibo Qiu[6], Chuanlai Shen[1,6*], Yuxian He[7*], Guangyu Zhao[2*]

[1]Department of Microbiology and Immunology, Medical School of Southeast University, Nanjing, Jiangsu, China 210009

[2]State Key Laboratory of Pathogen and Biosecurity, Beijing Institute of Microbiology and Epidemiology, Beijing, China 100071

[3]Blood Component Preparation Section, Jiangsu Province Blood Center, Nanjing, Jiangsu, China 210042

[4] Institute of Nephrology, Zhongda Hospital, Medical School of Southeast University, Nanjing, Jiangsu, China 210009

[5] Life Science & Technology School of Southeast University, Nanjing, Jiangsu, China 210096

[6]Jiangsu Province Key Laboratory of Critical Care Medicine, Department of Critical Care Medicine, Zhongda Hospital, Medical School of Southeast University, Nanjing, Jiangsu, China 210009

[7]Institute of Pathogen Biology, Chinese Academy of Medical Sciences and Peking Union Medical College, Beijing, China 100730

Running title: T cell epitopes of SARS-CoV-2 and induction of $CD8^+$ T cell responses

# These authors have equal contributions to this work.

* Corresponding authors:

Chuanlai Shen: chuanlaishen@seu.edu.cn; Yuxian He: yhe@ipb.pumc.edu.cn;

Guangyu Zhao: guangyu0525@163.com

bioRxiv preprint doi: https://doi.org/10.1101/2021.04.01.438020; this version posted May 24, 2021. The copyright holder for this preprint (which was not certified by peer review) is the author/funder. All rights reserved. No reuse allowed without permission.

Abstract

While SARS-CoV-2-specific T cells have been characterized to play essential roles in host immune protection in COVID-19 patients, few researches focus on the functional validation of T cell epitopes and development of vaccines inducing specific T cell responses. In this study, 120 $CD8^+$ T cell epitopes from E, M, N, S and RdRp proteins were validated. Among them, 110 epitopes have not been reported previously; 110, 15, 6, 14 and 12 epitopes were highly homologous with SARS-CoV, OC43, NL63, HKU1, and 229E, respectively; 4 epitopes from S protein displayed one amino acid distinct from the current variants of SARS-CoV-2. Thirty-one epitopes restricted by HLA-A2 molecule were used to generate peptide cocktail vaccines in combination with Poly(I:C), R848 or polylactic-co-glycolic acid nanoparticles, which elicited robust specific $CD8^+$ T cell responses in wild-type and HLA-A2/DR1 transgenic mice. Seven of the 31 epitopes were found to be cross-presented by HLA-A2 and H-2K/D^b molecules. Unlike previous researches, this study established a modified cell co-culture system of DC-peptide-PBL using healthy donor's PBMCs to validate the $CD8^+$ T cell epitope on-silicon predicted; provided a library of $CD8^+$ T cell epitopes restricted by a series of high-frequency HLA-A allotypes which covering broad Asian populations; identified the HLA-A cross-restrictions of these $CD8^+$ T cell epitopes using competitive binding experiments with HMy2.CIR cell lines expressing indicated HLA-A molecules; and initially confirmed the *in vivo* feasibility of 9 or 10-mer peptide cocktail vaccines of SARS-CoV2. These data will facilitate the development of vaccines inducing antiviral $CD8^+$ T cell responses.

Key words： SARS-CoV-2; T cell epitope; HLA-A; Vaccine

bioRxiv preprint doi: https://doi.org/10.1101/2021.04.01.438020; this version posted May 24, 2021. The copyright holder for this preprint (which was not certified by peer review) is the author/funder. All rights reserved. No reuse allowed without permission.

Introduction

The highly contagious COVID-19 has spread worldwide at an unprecedentedly quick speed since its first identification at December 2019, leading to an ongoing global pandemic[1]. As 22 of April, 2021, there have been more than 143 million confirmed cases and over 3.0 million deaths. Although relentless efforts have been paid in effective vaccine race, there are still many risks for a long-term immune protection[2], since host immunity to Severe Acute Respiratory Syndrome Coronavirus 2 (SARS-CoV-2) has not been fully understood. Currently, most vaccines focus on the induction of neutralizing antibodies against spike (S) protein of SARS-CoV-2 [3, 4], which can block the virus from entering and infecting human cells, helping the immune system to clear the virus and to prevent future infections[5]. However, researchers have found that circulating antibodies to SARS-Cov-2 declined rapidly and persisted only around seven months. And, certain patients who are asymptomatic or mildly symptomatic do not have detectable neutralizing antibodies[6]. In addition, growing incidence of COVID-19 re-infections emerges since the first reported re-infection in August, 2020. This suggests that neutralizing antibodies cannot offer long-term protection. Furthermore, SARS-CoV-2 constantly undergoes mutations as it spread from person to person. Therefore, more studies are needed to determine whether the current vaccines will be still effective against the virus quasispecies.

It has been studies that T cells, especially $CD8^+$ T cells, also play a critical role in the defense of many viral infections[7]. Increasing evidences indicate that T cell responses are important in the immune response against SARS-CoV-2, and may mediate long-term protection[8-12]. The specific T cells showed a highly activated cytotoxic phenotype in the acute

bioRxiv preprint doi: https://doi.org/10.1101/2021.04.01.438020; this version posted May 24, 2021. The copyright holder for this preprint (which was not certified by peer review) is the author/funder. All rights reserved. No reuse allowed without permission.

74 phase that correlated with various clinical markers of disease severity, whereas the
75 convalescent-phase specific T cells were multifunctional and showed a stem cell-like memory
76 phenotype in the mild and asymptomatic patients[12-19]. Moreover, intensive expansion of
77 highly cytotoxic T cells was associated with convalescence in moderate patients[19].
78 SARS-CoV-2-specifific T cells were detectable in antibody-seronegative exposed family
79 members and convalescent individuals with a history of asymptomatic and mild COVID-19[12].
80 As a result, T cell immunity would be critical in the pathogenesis and immune protection
81 mechanism of COVID-19, thus providing a potential way to develop long-term effective
82 vaccines and treatments[20]. However, thus far limited information is available about the
83 vaccines inducing T cell immune protections against SARS-CoV-2. Very recently,
84 SARS-CoV-2 T cell epitopes restricted by H-2^{d} and H-2^{b} molecules were identified, and three
85 of which were used to generate the venezuelan equine encephalitis replicon particles (VRP)
86 expressing single T cell epitope[21]. This VRP vaccine induced robust CD4^{+} or CD8^{+} T cell
87 responses, which mediated more rapid viral clearance than neutralizing antibodies and
88 decreased the extent of lung pathological changes in Ad5-ACE2-tranduced and
89 SARS-CoV-2-infected mice[21], indicating the potential of T cell epitope vaccine. In addition,
90 HLA-DR-restricted peptides cocktail vaccine from Tubingen University of Germany has been
91 enrolled in phase I clinical trial (NCT04546841). Whether the 9- or 10-mer peptides cocktail
92 restricted by HLA class I molecule can induce SARS-CoV-2 sepcific CD8^{+} T cell responses *in*
93 *vivo* remains unknown.

94 Identification of T cell epitopes in SARS-CoV-2 proteins can contribute greatly to the
95 development of T cell epitope vaccines and precise evaluation of host cellular immunity.

bioRxiv preprint doi: https://doi.org/10.1101/2021.04.01.438020; this version posted May 24, 2021. The copyright holder for this preprint (which was not certified by peer review) is the author/funder. All rights reserved. No reuse allowed without permission.

However, most studies have utilized pools of predicted or overlapping peptides spanning the sequences of different SARS-CoV-2 proteins [22-28]. The functionally validated T cell epitopes are still limited and have thus far come from only a few laboratories[10, 11, 29-32]. These T cell epitopes are presented only by several HLA class I or II molecules and the precise HLA restrictions of each epitope needs to be further defined.

To screen more $CD8^+$ T cell epitopes which cover more predominant HLA-A allotypes and more SARS-CoV-2 proteins, here we dedicated to the mapping of HLA-A-restricted epitopes from envelope proteins (E), membrane protein (M), nucleocapsid protein (N), spike glycoprotein (S) and RNA-dependent RNA polymerase (RdRp) of SARS-CoV-2. Four hundred and nine epitopes, which restricted by nine high-frequency HLA-A allotypes, were on-silicon predicted and selected. Then the immunogenicity and HLA-A cross-restrictions of 120 epitopes were validated by DC-peptide-PBL co-culture experiments using healthy donors' PBMCs and competitive binding experiments with HMy2. CIR cell lines expressing indicated HLA-A molecules. Thirty-one epitope peptides restricted by HLA-A2 molecule were used to generate the 9- or 10-mer peptide cocktail vaccines in combination with Poly(I:C), R848 or polylactic-co-glycolic acid nanoparticles (PLGA-NPs), which induced robust SARS-CoV-2 specific $CD8^+$ T cell responses in HLA-A2/DR1 transgenic mice and wild-type mice.

Results

1. HLA-A restricted 409 T cell epitopes were on-silicon predicted and selected from SARS-CoV-2 proteins

SARS-CoV-2 T cell epitopes, which restricted by nine high-frequency HLA-A allotypes

bioRxiv preprint doi: https://doi.org/10.1101/2021.04.01.438020; this version posted May 24, 2021. The copyright holder for this preprint (which was not certified by peer review) is the author/funder. All rights reserved. No reuse allowed without permission.

(HLA-A*02:01, A*11:01, A*24:02, A*02:06, A*02:07, A*33:03, A*30:01, A*02:03, or A*11:02) with the total gene frequency of around 87% in Chinese population (http://www.allelefrequencies.net), were predicted from four structural protein (E, M, N, S） and one non-structural protein (RdRP) using five epitope predication tools (IEDB-ANN, IEDB-SMM, SYFPEITHI, EPIJEN, NetMHC and ConvMHC). For each HLA-A molecule and each protein, one to twenty 9- or 10-mer peptides with the highest score (highest affinity) were selected as candidate epitopes. A total of 409 peptides restricted by indicated HLA-A molecules were finally selected as candidate epitopes with the number of 45, 63, 71, 130, and 100 from E, M, N, S and RdRp proteins, respectively. Among them, 139 indicated epitopes are common or highly homologous epitopes cross-presented by several HLA-A molecules, thus finally only 270 indicated candidate epitope peptides (9-mer or 10-mer) were synthesized for further identification (Table S1).

2. Immunogenicity of 120 candidate epitopes was validated by DC-peptide-PBL co-culture experiments

In order to validate the immunogenicity of candidate epitopes, PBMCs from healthy blood donors were collected and HLA-A alleles were identified. DCs were induced for 7 days and then coincubated with candidate epitope peptides and autologous PBL for 14 days. Cells were harvested and stimulated by corresponding candidate peptides for another 16 hours followed by IFN-γ intracellular staining (ICS) and flow cytometry. In some DC-peptide-PBL co-culture wells, the autologous PBLs were prelabeled with CFSE. After 14-day co-cultures, the cells were harvested followed by flow cytometry to detect the proliferation percentage of $CD8^+$ T cell. When the frequency of IFN-γ^+ T cells in $CD3^+/CD8^+$ T cell population increased by more

bioRxiv preprint doi: https://doi.org/10.1101/2021.04.01.438020; this version posted May 24, 2021. The copyright holder for this preprint (which was not certified by peer review) is the author/funder. All rights reserved. No reuse allowed without permission.

than 100% compared with the negative control or proliferation percentage of $CD8^+$ T cells in $CD3^+/CD8^+$ T cell population increased by more than 20% compared with the negative control, the candidate epitope peptide in the co-culture well was identified as positive peptide with immunogenicity.

To evaluate whether this procedure is sensitive for identification of peptide immunogenicity, several reference peptides were tested using this DC-peptide-PBL co-culture procedure. These HLA-A restricted T cell epitopes derived from hepatocellular carcinoma (HCC)-associated tumor antigens (HCC 1-1, HCC 1-2, HCC 5-3, HCC 5-4, HCC 5-5) or from hepatitis B virus antigens (HBV 111, HBV 118) have been validated as real-world epitopes previously in-house by using HCC patients' PBMCs or chronic hepatitis patient's PBMCs (manuscript submitted). They can effectively stimulate the patient's fresh PBMCs to produce IFN-γ in *ex vivo* 20-hour co-culture as detected by ELISPOT assay. Here, they were also defined as positive peptides in DC-peptide-PBL co-cultures using healthy donor's PBMCs as detected by intracellular IFN-γ staining and CFSE proliferation analyses, meanwhile the weak positive reference peptides (HCC 1-1, HCC 1-2) were defined as negative peptides here (Figure 1).

After the PBMC samples from 156 healthy donors were tested, a total of 120 candidate epitope peptides of SARS-CoV-2 have been defined as antigenic T cell epitopes by using the DC-peptide-PBL procedure, which indicating that they can elicit naive peptide-specific $CD8^+$ T cells to activate and produce IFN-γ or proliferate after 14 days co-stimulation. Some candidate epitope peptides have been validated in several healthy donor' PBMCs. 110 of 120 positive epitopes have not been reported previously. The detailed data of all positive peptides

bioRxiv preprint doi: https://doi.org/10.1101/2021.04.01.438020; this version posted May 24, 2021. The copyright holder for this preprint (which was not certified by peer review) is the author/funder. All rights reserved. No reuse allowed without permission.

were summarized in Table 1. Of them, the number of epitopes derived from E (75aa), M (222aa), N (419aa), S (1273aa) and RdRp (932aa) proteins is 18, 27, 12, 36, and 27, respectively, with a relatively bias distribution. The density of $CD8^+$ T cell epitopes per 10 aa is 2.40, 1.216, 0.286, 0.283, and 0.290, respectively. Their sequence homology between SARS-CoV-2 and other HCoVs were aligned and exhibited in Table S2. Of the 120 validated SARS-CoV-2 $CD8^+$ T cell epitopes, 110, 15, 6, 14 and 12 epitopes were highly homologous (0-2 amino acids deviation) with SARS-CoV, OC43, NL63, HKU1,and 229E, respectively. The common epitopes with common-cold HCoVs mainly locate in RdRp protein (39/47). In addition, 4 epitopes displayed one amino acid distinct from the current mutant variants, such as D50 and D82 for B.1.1.7, D82 for B.1.351 and P.1, D78 for B.1.617, and D53 for Denmark Variant (Table S2).

Figure S1 showed the phenotypes of mature DC as verified by flow cytometry. Figure 2 presented the IFN-γ ICS flow plots and $CD8^+$ T cell proliferation flow plots of partial positive peptides. All flow plots of 120 positive peptides were displayed in Figure S2 and S3.

3. **Binding affinity and cross-binding of positive epitope peptides with HLA-A allotypes**

HMy2.CIR is a human B lymphocyte strain with HLA class I antigen deficiency, which does not express HLA-A and B molecules and only expresses trace HLA-Cw4. To assess the affinity of the positive peptides with the corresponding HLA-A molecules, the transfected HMy2.CIR cell lines expressing indicated HLA-A molecules (HLA-A2402, A0203, A0201, A0206, A1101, A3303, A0101, or A3001) were generated firstly, sorted by flow cytometry, and identified by sequencing. The purity of these transfected CIR cell lines after sorting was 80% to 94% (Figure S4).

bioRxiv preprint doi: https://doi.org/10.1101/2021.04.01.438020; this version posted May 24, 2021. The copyright holder for this preprint (which was not certified by peer review) is the author/funder. All rights reserved. No reuse allowed without permission.

Then, the unlabeled positive peptides of SRAS-CoV-2 competed with fluorescent-labeled reference peptides for binding with the corresponding HLA-A molecules onto indicated transfected cell lines for 24 hours. As the FACS data showed, most positive peptides could result in a left shift of the fluorescent peak of reference peptide (Figure S5). According to the IC50, peptides were classified into three categories. Binding affinity was high when IC50 was less than 5 μM, intermediate when between 5 μM and 15μM, and low or no binding when more than 15 μM. Table 2 exhibited the binding affinity of each tested peptides with associated HLA-A molecules. These data also revealed the cross-binding of indicated peptide with different HLA-A allotypes (Table 3). Surprisingly, all epitopes derived from E protein displayed low affinity with corresponding HLA-A allotypes in this HLA-A competitive binding assay (Table 3), but these data are inconsistent with the results from DC-peptide-PBL costimulation and vaccine immunization in HLA-A2/DR1 transgenic mice.

4. The peptide cocktail vaccines induced robust specific $CD8^+$ T cell responses in HLA-A2/DR1 transgenic mice

To determine whether these peptides which was validated by DC-peptide-PBL co-culture experiments can stimulate T cell responses *in vivo*, 31 positive epitope peptides restricted by HLA-A2 molecule (HLA-A0201, A0203, A0206, A0207) were grouped into 4 peptide pools (Table S3) and were used to generate peptide cocktail vaccines in three formulations: the peptides-encapsulated and -surface coupled PLGA-NPs/peptides (Vaccine A), R848/peptides (Vaccine B), and poly I:C/peptides (Vaccine C) (Table S4). Additionally, T2 cell binding assay was used to define the affinity of the 31 epitopes with HLA-A0201 molecule. T2 cells were incubated with indicated peptide or no peptide and β2-microglobulin

bioRxiv preprint doi: https://doi.org/10.1101/2021.04.01.438020; this version posted May 24, 2021. The copyright holder for this preprint (which was not certified by peer review) is the author/funder. All rights reserved. No reuse allowed without permission.

for 16 hours. Then, peptide-induced up-regulation of HLA-A0201 expression on T2 cells was measured by PE-labeled anti-HLA-A2.1 antibody staining and flow cytometry (Figure S6). According to the fluorescence index (FI), 18 epitopes showed high affinity (FI > 1.0), 7 epitopes displayed intermediate affinity (1.0 ≥ FI >0.5), and 6 epitopes exhibited low or no binding (FI ≤ 0.5) with HLA-A0201 molecules (Table S5). Finally, HLA-A0201$^{+/+}$/DR1$^{+/+}$ transgenic and H-2-β2m$^{-/-}$/I-Aβ$^{-/-}$ C57BL/6 mice were immunized with the three vaccines respectively. After three rounds *in vivo* stimulation, splenocytes of primed mice were tested for peptide-specific T cell responses by IFN-γ-ELSPOT, IFN-γ-ICS and IFN-γ-ELISA.

The 31 positive peptides were grouped into eight pools (Table S3) according to their derived proteins and the features of acid and alkalinity. Then splenocytes from each mouse were coincubated with each peptides pool or PBS for 20 hours in 96-well PVDF membrane plate and followed by IFN-γ-ELSPOT assay. The total spot forming unit (SFU) in 2×10^5 splenocytes from each mouse in the three vaccine groups was 400-500 times more than that from control group (Figure 3A). Interestingly, splenocytes in all vaccine groups showed almost the strongest T cell responses to E protein and weakest T cell responses to N protein relative to other antigens (Figure 3B). Figure 4 presented the spots of ELISPOT assay from all mice. Two irrelevant CD8$^+$ T cell epitope peptides (AFP$_{158\text{-}166}$ and AFP$_{424\text{-}432}$) were used as antigen-irrelevant control groups and obtained the negative results similar to that in no peptide group.

To further confirm the results from ELISPOT assay and the specific CD8$^+$ T cell responses, IFN-γ intracellular cytokine staining was performed. The 31 positive peptides were grouped into five pools (Table S3) according to their derived proteins. Then splenocytes from

bioRxiv preprint doi: https://doi.org/10.1101/2021.04.01.438020; this version posted May 24, 2021. The copyright holder for this preprint (which was not certified by peer review) is the author/funder. All rights reserved. No reuse allowed without permission.

each mouse were coincubated with each peptides pool or PBS for 16 hours in 48-well plate and followed by another 6 hours coincubation with BFA/Monensin mixture. The resulting ICS showed that the frequencies of IFN-γ^+ in $CD3^+CD8^+$ T cell populations from the three vaccine groups were about 20-30 times higher than that in control mice (Figure 3C). Splenocytes in vaccine A group showed the strongest $CD8^+$ T cell responses to RdRP while splenocytes in vaccine C group showed the strongest $CD8^+$ T cell responses to E protein (Figure 3D). Figure 5 presented the flow plots for ICS from all mice. Also, two irrelevant $CD8^+$ T cell epitope peptides ($AFP_{158\text{-}166}$ and $AFP_{424\text{-}432}$) were used and obtained the results similar to the no peptide group.

Furthermore, ELISA was carried out to quantify IFN-γ in the supernatant after the splenocytes were incubated with each of the five peptide pools or PBS in 48-well plate for 72 hours. Accumulations of IFN-γ in the supernatant of the three vaccine groups were about 15-30 times higher than that in control group (Figure 6A), which is consistent with the results of ELISPOT and ICS. Splenocytes in all three vaccine groups showed relatively stronger responses to RdRP protein (Figure 6B).

Taken together, these results indicated that all three forms of epitope peptide cocktail vaccines can stimulate robust specific $CD8^+$ T cell responses in HLA-A2/DR1 transgenic mice, implying the potential of these validated SARS-CoV-2 T cell epitopes to be applied in vaccine development. Of note, the mouse-3 in Vaccine B group (R848/peptide vaccine) showed only weak or no T cell responses as detected by ELSPOT, ICS and ELISA. This failure may be due to the weak reactivity of entire T cell repertoire since the SFU of 2×10^5 splenocytes was much less than other primed mice after stimulated by mitogen PHA as

bioRxiv preprint doi: https://doi.org/10.1101/2021.04.01.438020; this version posted May 24, 2021. The copyright holder for this preprint (which was not certified by peer review) is the author/funder. All rights reserved. No reuse allowed without permission.

250 detected by ELISPOT (70 vs. 832.2 ± 328.9). In order to further confirm the *in vivo* results,
251 Vaccine C (poly I:C/peptides) immunization experiment was repeated in the
252 HLA-A0201$^{+/+}$/DR1$^{+/+}$ transgenic and H-2-β2m$^{-/-}$/I-Aβ$^{-/-}$ C57BL/6 mice and induced similar
253 trend of robust CD8^{+} T cell responses compared to control group.

254 **5. The peptide cocktail vaccine induced CD8^{+} T cell responses in wild-type C57BL/6**
255 **mice**

256 To investigate whether the HLA-A2 molecules-restricted 9 or 10-mer peptides can also be
257 cross-presented by mouse H-2K/D^{b} molecules, the wild-type C57BL/6 mice were immunized
258 with vaccine C (peptide pool-v1, pool-v2, pool-v3 and pool-v4 mixed with poly I:C). After
259 three rounds of *in vivo* stimulation according to the timeline in HLA-A2/DR1 transgenic mice,
260 splenocytes from primed C57BL/6 mice were detected by ICS. The frequencies of IFN-γ^{+} T
261 cells in CD3^{+}/CD8^{+} populations were 4-7 times higher in the 2 of 4 vaccination mice than that
262 in the control group (Figure 6C). The robust CD8^{+} T cell responses were mainly against the
263 epitopes from M, N and S protein (Figure 6D). Figure 7A presented the flow plots of all mice.
264 Also, two irrelevant CD8^{+} T cell epitope peptides (AFP$_{158\text{-}166}$ and AFP$_{424\text{-}432}$) were used and
265 obtained the results similar to the no peptide group.

266 To further identify the epitopes cross-presented by mouse H-2K/D^{b} molecules, the
267 splenocytes from primed Vaccine mouse-2 and Vaccine mouse-3 were coincubated with each
268 of the 31 positive epitope peptides and followed by ICS. Flow cytometric data showed that 7
269 of 31 epitope peptides (A5, B1, B2, B6, C2, D6 and D13) can activate the primed splenocytes
270 with a frequency of IFN-γ^{+} T cells in CD3^{+}/CD8^{+} population two times higher than that of no
271 *ex vivo* stimulation group (Figure 7B).

bioRxiv preprint doi: https://doi.org/10.1101/2021.04.01.438020; this version posted May 24, 2021. The copyright holder for this preprint (which was not certified by peer review) is the author/funder. All rights reserved. No reuse allowed without permission.

6. T cell epitope-based peptide cocktail vaccines do not lead to visible organ toxicity

To uncover whether the peptide-based vaccine immunizations cause organ toxicity, the heart, liver, lung and kidney from each mouse were checked at day 28 after the mice were inoculated three times with Vaccine A, Vaccine B or Vaccine C. The organs were immersed and stained with Hematoxylin-Eosin. As the scanning copy showed, no visible organ toxicity was found in all organs in each group (Figure S7).

Discussion

SARS-CoV-2 has seriously hazarded public health and the economic development all over the word. Many people are suffering from the physical symptoms or the adverse impacts caused by this major epidemic disease. Despite of great efforts made by scientists around the world, the epidemic situation is still out of control. COVID-19 vaccine development is of major importance, but mainly biased towards neutralizing antibody protection with generally less effective at eliciting $CD8^+$ T cell responses, which faces possible risk in clearing virus and in preventing from infection. Informed by protective immunity observed in natural infection, people have known that vaccine approaches that elicit antiviral SARS-CoV-2 specific $CD4^+$ and $CD8^+$ T cells in coordination with neutralizing antibodies will generate more robust and durable protective immunity[20, 33]. As known, memory T cell responses can persist for 6-17 years after SARS-CoV infection[10, 34] and, in mice, protect against lethal virus challenge[35]. In contrast, memory B cells live short in host[34, 35].

However, only several reports are thus far available about the vaccine candidate T cell epitopes that have been validated by functional experiments. 408 $CD8^+$ T cell epitopes

bioRxiv preprint doi: https://doi.org/10.1101/2021.04.01.438020; this version posted May 24, 2021. The copyright holder for this preprint (which was not certified by peer review) is the author/funder. All rights reserved. No reuse allowed without permission.

294 on-silicon predicted were applied in multiplexed peptide-MHC tetramer staining to detect the
295 PBMCs from 30 convalescent COVID-19 patients, then 132 positive reactions were obtained
296 with the validation of 42 $CD8^+$ T cell epitopes presented by 6 HLA allotypes (HLA-A0101,
297 A0201, A0301, A1101, A2402 and B0702)[32]. Prackar et al tested the binding stability of 777
298 $CD4^+$ and $CD8^+$ T cell epitopes that were predicted to be good binders across 11 MHC
299 allotypes using an *in vitro* peptide MHC stability assay, and found that 174 peptides can stably
300 bind to the HLA allotypes (HLA-A0101, A0201, A0301, A1101, A2402, B4001, C0102,
301 C0401, C0701, C0702, DRB10401), of which 126 have not been reported previously[31]. After
302 14-day cocultures of predicted epitope pools with PBMCs from healthy individuals, 142
303 $CD4^+$ T cell epitopes were defined by immunofluorescence spot assay (FluoroSpot)[30].
304 Furthermore, using genome-wide screening technology (T-Scan), 29 $CD8^+$ T cell epitopes
305 were identified, and presented by 6 different HLA allotypes (A0201, A0101, A0301, A1101,
306 A2402, B0702)[29]. Thus far, the validated SARS-CoV-2 T cell epitopes, especially $CD8^+$ T cell
307 epitopes, are still limited and few epitopes have been used *in vivo* as vaccines. More
308 importantly, these validated epitopes are only presented by a few HLA allotypes which can
309 not cover a broad population in indicated geographical regions. This may hamper the
310 development of T cell epitope vaccines and the precise evaluation on herd cellular immune
311 protection.

312 Unlike the previous researches about T cell epitopes of SARS-CoV-2, this study has four
313 points of worth noting. First, this study focus on a series of high-frequency HLA-A allotypes
314 which gather a total HLA-A allele frequency of around 87% in Chinese population while 79%,
315 78%, 63%, 59.5%, 49.5% and 46.5% in Southeast Asia, Northeast Asia, Indonesia, South

bioRxiv preprint doi: https://doi.org/10.1101/2021.04.01.438020; this version posted May 24, 2021. The copyright holder for this preprint (which was not certified by peer review) is the author/funder. All rights reserved. No reuse allowed without permission.

316 America, Europe and North America populations, respectively
317 (http://www.allelefrequencies.net). Since T cell epitopes spread across the proteome of
318 SARS-CoV-2 in a relatively equal distribution[9], here four structural proteins and the RdRp
319 consisted of nsp7, nsp8 and nsp12 were screened for the identification of $CD8^+$ T cell epitopes
320 cross-restricted by the high-frequency HLA-A allotypes. This study has provided a library of
321 $CD8^+$ T cell epitopes that not only covers broad antigenic targets recognized by
322 SARS-CoV-2-specific $CD8^+$ T cell clones, but also fits to the Asian herd genetic
323 characteristics of HLA molecules, thus will facilitate the development of SARS-CoV-2
324 vaccines inducing antiviral $CD8^+$ T cell responses for Asian populations.

325 Second, this study established a modified cell co-culture system of DC-peptide-PBL
326 using healthy donor's PBMCs to validate the immunogenicity of $CD8^+$ T cell epitope
327 on-silicon predicted. The most reliable and valuable method to validate the immunogenicity
328 of candidate T cell epitopes is the detection of epitope-specific memory T cell clones in the
329 PBMCs or other cell samples from COVID-19 patients or convalescent humans. However, it
330 is less practicable in current China due to the difficulty obtaining clinical blood samples. So,
331 an alternative approach using PBMCs from unexposed humans was used here. The DC-T or
332 peptide-PBMC co-culture procedures using healthy donor's PBMCs have been generally used
333 to validate the $CD4^+$ T cell epitopes by the exogenous antigen presenting mechanism[30]. In this
334 study, DC-T and peptide-PBMC experiments were integrated as DC-peptide-PBL
335 co-stimulation system, and initially applied for the validation of $CD8^+$ T cell epitopes. DCs
336 were induced from the healthy donors' PBMCs, and coincubated for 14 days with candidate
337 epitope peptides and autologous PBLs. In this co-culture system, the 9-mer or 10-mer

bioRxiv preprint doi: https://doi.org/10.1101/2021.04.01.438020; this version posted May 24, 2021. The copyright holder for this preprint (which was not certified by peer review) is the author/funder. All rights reserved. No reuse allowed without permission.

peptides are maintained in culture media at a high concentration of 20 μg/mL during 14 days, and may be engulfed by DCs and cross-presented to $CD8^+$ T cell by HLA-A molecules, or directly bind to the HLA-A molecules onto DCs and B cells followed by activation of naive $CD8^+$ T cells or SARS-CoV-2 cross-reactive memory $CD8^+$ T cells. This presumption was verified at least in part by the positive results of DC-peptide-PBL experiments in this study. Many candidate epitope peptides can increase the frequency of IFN-γ^+ $CD8^+$ T cells by 3-5 times in this co-culture system. Compared with the ICS, the detection of $CD8^+$ T cell proliferation by using CSFE-prelabeled PBLs is less sensitive. Of note is that the healthy donor's DC-T *in vitro* co-cultures usually can increase peptide-specific $CD4^+$ T cells by around 10 times since the exogenous antigen procession and presentation mechanism[30]. More interestingly, 44 (36.66%) of the 120 validated $CD8^+$ T cell epitope peptides can also simultaneously activate $CD4^+$ T cells with the 2-6 times increase of IFN-γ^+/$CD4^+$ T cell frequency or $CD4^+$ T cell proliferation (data not shown). The underlying mechanism remains to be further elucidated.

In order to further confirm the sensitivity and reliability of this co-culture system, some reference $CD8^+$ T cell epitope peptides, which were derived from HCC-associated tumor antigens or from hepatitis B virus antigens and have been validated as real-world epitopes previously in-house by using HCC patients' PBMCs or chronic hepatitis patient's PBMCs, were tested in this system and achieved positive results. In addition, HLA-A molecule competitive binding experiments also were used to confirm the binding affinity of the 120 positive peptides with corresponding HLA-A molecules onto HMy2.CIR cell lines. The results are mostly consistent in that of DC-peptide-PBL experiments except the epitopes

bioRxiv preprint doi: https://doi.org/10.1101/2021.04.01.438020; this version posted May 24, 2021. The copyright holder for this preprint (which was not certified by peer review) is the author/funder. All rights reserved. No reuse allowed without permission.

derived from E protein, and further identified the HLA-A restrictions and cross-restrictions of each epitope peptides. Furthermore, the robust $CD8^+$ T cell responses elicited by the HLA-A2-binding peptide cocktails in HLA-A2/DR1 transgenic mice also indicated the *in vivo* immunogenicity of representative epitope peptides validated by this DC-peptide-PBL procedure.

For this study, the third point different from previous researches is that the HLA-A cross-restrictions of 120 positive $CD8^+$ T cell epitopes were further identified by using HLA-A molecule competitive binding experiments with HMy2.CIR cell lines expressing indicated HLA-A molecules. As known, one T cell epitope can be presented by several HLA allotypes with distinct binding affinity. The HLA molecule restrictions and cross-restrictions of most SARS-CoV-2 T cell epitopes previously reported have not been elucidated, but only have been affirmed by on-silicon prediction and mere guesswork according to the donor's HLA allele genotypes[29, 30, 32].

More importantly, this study initially confirmed the *in vivo* feasibility of 9 or 10-mer peptide cocktail vaccines of SARS-CoV2. As known, HLA class II molecule restricted peptides (15 or 16-mer long) can induce $CD4^+$ T cell responses *in vivo*. For SARS-CoV2, HLA-DR restricted peptides cocktail vaccine from Tubingen University of Germany has been enrolled in phase I clinical trial (NCT04546841). However, few 9-mer or 10-mer $CD8^+$ T cell epitope peptides have been directly used *in vivo* as peptide vaccines. For tumor immunotherapy, tumor neoantigen peptide vaccines and mRNA vaccines have recently achieved robust T cell responses and encouraging clinical outcome[36, 37]. In clinical trials of melanomas[38, 39] and non-small cell lung cancers[40], the survival of patients was significantly

bioRxiv preprint doi: https://doi.org/10.1101/2021.04.01.438020; this version posted May 24, 2021. The copyright holder for this preprint (which was not certified by peer review) is the author/funder. All rights reserved. No reuse allowed without permission.

prolonged and the recurrence rate was reduced. Patrick A. Ott[38] identified up to 20 neoantigen peptides restricted by HLA-A or B allotypes from each melanoma patient using whole-exome sequencing of matched tumor and normal cell DNA and RNA sequencing of the tumor. Herein, the long peptides (with the length of 15–30 amino acids containing individual $CD8^+$ T cell epitope) rather than 9-mer or 10-mer peptides were synthesized and mixed with TLR3 agonist poly-ICLC to generate personal tumor neoantigen peptide vaccines. Of 6 vaccinated melanoma patients, 4 had no recurrence at 25 months post-vaccination, while 2 with progressive disease were subsequently treated with anti-PD-1 therapy and experienced complete tumor regression. The long peptide vaccines elicited expansion of the repertoire of neoantigen-specific T cells in each patient, but most were $CD4^+$ T cells rather than $CD8^+$ T cells. In this study, 31 short peptides of SARS-CoV-2 $CD8^+$ T cell epitope (with the length of 9-10 amino acids) were synthesized and mixed with R848, poly (I:C) or PLGA-NPs followed by immunizations in HLA-A2/DR1 transgenic mice and WT mice. The resulting data, for the first time to our knowledge, provide the experimental evidences that human MHC class I molecule-restricted short peptide cocktail vaccines can induce robust SARS-CoV2 specific $CD8^+$ T cell responses *in vivo*.

Using patients' PBMCs could only test whether the candidate peptide can be recognized by memory T cells *ex vivo*, while using healthy donor' PBMCs only test whether the candidate peptides can elicit naïve T cells *in vitro*. Whether the candidate peptide is also able to activate naïve T cells *in vivo* is a better criterion to judge it as an ideal vaccine candidate peptide. As compared with the Ad5-ACE2-transduced and SARS-CoV-2-infected BALB/c and C57BL/6 mice[21], HLA transgenic mice integrated with human HLA class I and II alleles

bioRxiv preprint doi: https://doi.org/10.1101/2021.04.01.438020; this version posted May 24, 2021. The copyright holder for this preprint (which was not certified by peer review) is the author/funder. All rights reserved. No reuse allowed without permission.

are more suitable for preclinical study of the vaccine. HLA-A*02:01 is one of the most common HLA class I alleles in the world, thus HLA-A*02:01 transgenic mice (HHD mice) have been generally used in identifying HLA-A0201-restricted epitopes and in evaluating peptide vaccines [41-43]. Herein, the HLA-A0201$^{+/+}$/DR1$^{+/+}$/H-2-β_2m$^{-/-}$/IA$\beta^{-/-}$ C57BL/6 mice were used in which the 9-mer or 10-mer peptides cocktail vaccines only can be presented by HLA-A2 or DR1 molecules, not by any H-2^b molecules, which indicated that this mouse model is more suitable to mimic the in-human antigen procession and presentation mechanism, without the interference caused by mouse H-2 molecules presentation. However, similar to the DC-peptide-PBL co-culture system, the detailed *in vivo* mechanism by which the exogenous 9 or 10-mer peptides elicit naive CD8$^+$ T cells activation remains unclear.

The 120 CD8$^+$ T cell epitopes spread across the E, M, N, S, and RdRp proteins of SARS-CoV-2 with a bias distribution. Notably, the shortest E protein presented the highest density of CD8$^+$ T cell epitope (2.400/10aa), two times relative to M protein (1.216/10aa), while N, S and RdRp proteins exhibited a similar low density (0.286, 0.283, 0.290 per 10aa) in this study. These data are discriminated with other findings in which T cell epitopes relatively equally distributed across the proteome of SARS-CoV-2[9].

Of the unexposed cohorts from the United States, Netherlands, Germany, Singapore, and United Kingdom, 20-50% could detect specific memory CD4$^+$ T cells that showed cross-reactivity to SARS-CoV-2 antigens, but the frequency was about 10 times lower (0.1% vs.1%) than that of those infected with SARS-CoV-2, presumably due to the common T cell epitopes between SARS-CoV-2 and common-cold HCoVs[8, 9, 30, 44]. In addition, long-lasting memory T cells reactive to N protein of SARS-CoV can be detected in 2020 in the

bioRxiv preprint doi: https://doi.org/10.1101/2021.04.01.438020; this version posted May 24, 2021. The copyright holder for this preprint (which was not certified by peer review) is the author/funder. All rights reserved. No reuse allowed without permission.

convalescent individuals with a history of SARS-CoV infection in 2003, and showed robust cross-responses against N protein of SARS-CoV-2[10]. In this study, depending on the sequence homologous alignment of SARS-CoV-2 with SARS-CoV, common-cold HCoVs, and current mutant variants of SARS-CoV-2, most epitopes (110) were common $CD8^+$ T cell epitopes of SARS-CoV. Additionally, 15, 6, 14 and 12 epitopes were also highly homologous (0-2 amino acids deviation) with OC43, NL63, HKU1, and 229E, respectively, which are mainly derived from in RdRp protein (39/47). These theoretical data support the previous findings in unexposed humans, but are contradictory with the previous research in which $CD8^+$ T cells generally do not cross-react with epitopes in the four common cold HCoVs[29]. Further detection using these homologous epitope peptides in unexposed cohort is needed. More importantly, of which 120 validated $CD8^+$ T cell epitopes of SARS-CoV-2, only 4 epitopes from S protein displayed one amino acid distinct from the five wide-spread virus variants while the one amino acid deviation at position 1, 3, 5 or 6 may or may not change epitope immunogenicity, suggesting the advantage of T cell epitope cocktail vaccine over the B cell epitope vaccine producing neutralizing antibody on the antiviral protections against mutant SARS-CoV-2.

In summary, 120 kinds of $CD8^+$ T cell epitopes derived from E, M, N, S, and RdRp proteins of SARS-CoV-2 and restricted by a series of high-frequency HLA-A allotypes were identified and validated. Among them, 110 and 47 epitopes are highly homologous with SARS-CoV and common-cold HCoVs respectively, 4 epitopes are distinct from current variants of SARS-CoV-2 with one amino acid substitution. HLA-A2-restricted 31 epitopes were generated as short peptide cocktail vaccines and triggered robust $CD8^+$ T cell responses

bioRxiv preprint doi: https://doi.org/10.1101/2021.04.01.438020; this version posted May 24, 2021. The copyright holder for this preprint (which was not certified by peer review) is the author/funder. All rights reserved. No reuse allowed without permission.

448 in HLA-A2/DR1 transgenic C57BL/6 mice and wild-type C57BL/6 mice. 7 epitopes were
449 found to be cross-presented by HLA-A2 and H-2K/D^b molecules. Whether these $CD8^+$ T cell
450 responses elicited by the peptides could facilitate virus clearance will be studies further.
451
452 **Materials and methods**
453 **1. Preparation of PBMCs and HLA-A gene typing**
454 The white blood cell filter trays after red blood cells preparation of healthy blood donors were
455 gotten from Blood Component Preparation Section of Jiangsu Province Blood Center. Then
456 white blood cells were collected from the white blood cell filter tray and PBMCs were
457 isolated by density-gradient centrifugation using Ficoll-Paque. The fresh PBMCs were either
458 used directly or cryopreserved in -80 ℃ until further test. HLA-A alleles were identified by
459 PCR-sequencing-based tying. The human samples collection and use has been approved by
460 Clinical Ethics Committee of Affiliated Zhongda hospital of Southeast University.
461 **2. Mice**
462 Female HLA-A*02:01/DR1 transgenic and H-2-$\beta_2m^{-/-}$/IA$\beta^{-/-}$ C57BL/6 mice at 10 weeks were
463 generous gifts from Academy of Military Medical Sciences. Female C57BL/6 mice at 10
464 weeks of age were purchased from the Comparative Medicine Center of Yangzhou University
465 (Yangzhou, China). Mice were maintained at the specific pathogen-free Animal Centre of
466 Southeast University (Nanjing, China). Animal welfare and experimental procedures were
467 performed in accordance with the Guide for the Care and Use of Laboratory Animals
468 (Ministry of Science and Technology of China, 2006) and were approved by the Animal
469 Ethics Committee of Southeast University.

bioRxiv preprint doi: https://doi.org/10.1101/2021.04.01.438020; this version posted May 24, 2021. The copyright holder for this preprint (which was not certified by peer review) is the author/funder. All rights reserved. No reuse allowed without permission.

3. On-silicon prediction of T cell epitopes and peptide synthesis

T cell epitopes spanning E, M, N, S, and RdRP proteins of SARS-CoV-2 (Wuhan strain) and presented by different HLA-A molecules were on-silicon predicted using five epitope predication tools and seven types of algorithms (IEDB-ANN, IEDB-SMM, SYFPEITHI, EPIJEN, NetMHC and ConvMHC). For each HLA-A molecule and for each protein, one to twenty 9-mer or 10-mer peptides with the highest score (highest affinity) as predicted by at least two tools were selected as candidate epitopes to be identified. The peptides were synthesized from China Peptides Co., Ltd with a purity above 95% defined by HPLC purification and mass spectrometry, and were used in cellular functional experiments. Lyophilized peptides were reconstituted at a stock concentration of 2mg/mL in DMSO-PBS solution.

4. DC-peptide-PBL co-culture experiment

Fresh PBMCs were suspended in serum-free RPMI 1640 and were allowed to adhere to culture flask for 2 hours in 5% CO_2 at 37℃. Non-adherent cells (PBLs) were then removed and were cryopreserved at -80℃ until further use. The resulting adherent cells were cultured in RPMI 1640 with 10% FCS, 1% penicillin/streptomycin, recombinant human GM-CSF (rhGM-CSF, 1000IU/mL, PrepoTech) and recombinant human IL-4 (rhIL-4, 500IU/mL, PrepoTech). At day 3 and day 5, half of the medium was replaced with fresh complete medium containing the cytokines with the same final concentration detailed above. At day 5, LPS (1μg/mL, sigma) was added to induce mature DCs (mDCs). At day 7, mature DCs (mDCs) were collected and were identified by flow cytometry (FACS Calibur, BD Bioscience) with FITC-labeled anti-CD83, anti-CD80, anti-CD86, anti-HLA-DR and PE-labeled

bioRxiv preprint doi: https://doi.org/10.1101/2021.04.01.438020; this version posted May 24, 2021. The copyright holder for this preprint (which was not certified by peer review) is the author/funder. All rights reserved. No reuse allowed without permission.

anti-HLA-ABC and anti-CD1a, respectively. mDCs were incubated with single peptide (20μg/mL, which corresponding to the HLA-A allele of indicated healthy donor) in serum free RPMI 1640 in 48-well plate (5×10^4 cells/well) for four hours in 5% CO_2 at 37℃, then the PBLs from the same donor (recovered one day ago, and prelabeled with CFSE or not) were added into the well (1×10^6 cells/well) for further 14-day co-culture. Recombinant human IL-2 (20 IU/mL) was added at day 11. At day 14, the corresponding peptide (20μg/mL) was added. At day 17, rhIL-2 was added again (10 IU/ mL). At day 21, cells were harvested and followed by ICS or T cell proliferation assay.

5. Intracellular IFN-γ staining of stimulated T cells

Cells from the DC-peptide-PBL co-cultures were harvested and coincubated with corresponding peptide (20μg/mL) or no peptide (negative control) for 16 hours in serum- free RPMI-1640 medium in 48-well plate at 37℃ and 5% CO2. After that, BFA/Monensin mixture was added to the cells for another 6 hours culture. Cells were then harvested, washed, blocked with human FcR Blocking Reagent (MACS) for 20 min at 4℃ and were stained with FITC-labeled anti-CD3 and APC-labeled anti-CD8 antibodies for 30 min at 4 ℃. After washing, cells were fixed and permeabilized following the protocol and were further incubated with PE-anti-human IFN-γ (4S.B3) (BD) for another 30 min at 4℃ followed by flow cytometry. The frequencies of IFN-γ^+ cells in $CD3^+/CD8^+$ populations were calculated.

6. **$CD8^+$ T cell proliferation assay**

In the DC-peptide-PBL co-culture, PBLs were pre-stained with CFSE. Briefly, PBLs were thawed, washed, and labeled with CFSE at a final concentration of 1.5μM for 20 min at 37℃. After washing, the CFSE-prelabeled PBLs were seeded into DC-peptide-PBL co-culture well

bioRxiv preprint doi: https://doi.org/10.1101/2021.04.01.438020; this version posted May 24, 2021. The copyright holder for this preprint (which was not certified by peer review) is the author/funder. All rights reserved. No reuse allowed without permission.

and incubated for 14 days. At day 22, cells were harvested and blocked with human FcR Blocking Reagent (MACS) for 20 min, then stained with PE-labeled anti-CD3 and APC-labeled anti-CD8 antibodies for 30 min at 4℃ for further analysis on the flow cytometry. The proliferation percentage of $CD8^+$ T cells in $CD3^+/CD8^+$ population was analyzed according to the reduction of CFSE-staining brightness.

7. Generation of HMy2.CIR cell lines expressing indicated HLA-A molecule

Total mRNA was extracted from the PBMCs of the healthy donor with indicated HLA-A alleles, the cDNA of each HLA-A allele was amplified using PCR and followed by the routine construction of pcDNATM3.1/myc-His(-)A recombinant plasmid. After electrotransfection, the cell lines stably expressing indicated HLA-A molecule was screened by G418. Then the cell lines were stained with fluorescence-labeled monoclonal antibody W6/32 against HLA-ABC or anti-HLA-A24, the high-expression cells were then sorted using flow cytometry and followed by pure culture and sequencing analyses.

8. **HLA-A molecule competitive binding assay**

A set of plasmid-transfected HMy2.CIR cell lines expressing indicated HLA-A molecule were generated in house and sorted by flow cytometry. The cell lines were then used in the competitive peptide binding assay according to the references[45]. Briefly, the CIR cell lines expressing indicated HLA-A molecule were washed with acid buffer (0.131M citric acid and 0.061M sodium phosphate Na_2HPO_4, PH3.3, 0.22μm filtered) for 1 min, and then neutralized by IMDM medium containing 0.5%BSA. Cells were washed, seeded into 96-well U culture plate (1×10^5 cells/100μL/well) with β_2-m (1μg/mL). Then 25μL unlabeled peptide to be tested (5μM or 15μM) and 25μL fluorescent-labeled reference peptide (300nM) were added into the

bioRxiv preprint doi: https://doi.org/10.1101/2021.04.01.438020; this version posted May 24, 2021. The copyright holder for this preprint (which was not certified by peer review) is the author/funder. All rights reserved. No reuse allowed without permission.

well and coincubated for 24h at 4℃. The reference peptides used in this research were FLPSDK(FITC)FPSV (for HLA-A0201, A0203 and A0206), YVNVNK(FITC)GLK (for HLA-A1101 and A3303), EYLVSK(FITC)GVW (for A2402), YLEPAK(FITC)AKY (for A0101) and ASRELK(FITC)VSY (for A3001). The plate was centrifuged at 600rpm for 5min at room temperature (RT). Cells were washed twice with 100μL cold 0.5% BSA-PBS. Finally, cells were resuspended with 150μL PBS and transferred to the flow tube and further analyzed with flow cytometry. Fluorescence polarization (FP) _sample is the FP value for the sample, while the minimum FP_ free is the FP value for free FITC-labeled reference peptide, and the maximum reaction FP_ no is the FP value for FITC-labeled reference peptide without unlabeled competitor peptide. Competitive binding (%) = [1-(FP_ sample-FP_ free) / (FP_ no -FP_ free)] × 100%. IC50 is the concentration of unlabeled peptide required to inhibit the binding of labeled reference peptide by 50%, which is calculated from the competitively binding inhibition (%) of the sample at 5μM and 15μM. Binding affinity of unlabeled peptide with indicated HLA-A molecule is assessed by IC50. IC50<5μM means high binding affinity, between 5-15μM means intermediate binding affinity, more than 15μM means low binding affinity or no binding affinity.

9. Preparation of peptide pools for vaccine immunization

Validated antigenic peptides restricted by HLA-A2 molecules (including A0201, A0203, A0206, A0207) were reconstituted in ideal solution before use at a final concentration of 5mg/mL for vaccine immunization and 2mg/mL for T cell response detection. Totally 31 antigenic peptides (9-mer or 10-mer) were grouped into four pools (pool-v1 to v4) for vaccine immunization (Table S3). For IFN-γ-ELISPOT assay, the 31 antigenic peptides were grouped

bioRxiv preprint doi: https://doi.org/10.1101/2021.04.01.438020; this version posted May 24, 2021. The copyright holder for this preprint (which was not certified by peer review) is the author/funder. All rights reserved. No reuse allowed without permission.

into eight pools according to their derived protein and the feature of acid and alkalinity (Table S3). For IFN-γ ICS and ELISA, the 31 antigenic peptides were grouped into five pools according to their derived proteins (Table S3).

10. T2 cell binding assay

To assess the affinity of HLA-A2-restricted epitope peptides with HLA-A0201 molecule, peptide-induced up-regulation of HLA-A0201 expression on T2 cells was measured. Briefly, T2 cells were incubated with single peptide of the 31 epitopes (50μg/mL) or CMVpp65$_{495\text{-}503}$ peptide (NLVPMVATV, 50μg/mL, as positive control) or OVA$_{257\text{-}264}$ peptide (SIINFKEL, 50μg/mL, as negative control) or no peptide and 3μg/mL β2-m for 16 hours at 37 ℃ and 5% CO_2. Then T2 cells were stained with PE-labeled anti-HLA-A2.1 antibody for 30 min at 4 ℃ followed by flow cytometry. The fluorescence index (FI) was calculated as follows: FI = (mean PE fluorescence with the given peptide - mean PE fluorescence without peptide)/ (mean PE without peptide). FI > 0.5 was the criteria of peptides with affinity while peptides with FI > 1 were regarded as high-affinity epitopes. FI ≤ 0.5 means low affinity or no binding.

11. Preparation of PLGA-NPs/peptides vaccine

Peptides-encapsulated PLGA-NPs were prepared freshly using the double-emulsion solvent evaporation method. To equal the amount of peptides in PLGA-NPs/peptides vaccine to the PolyI:C/peptides vaccine and R848/peptides vaccine, the loading efficiency of the PLGA-NPs was calculated before vaccination, then the PLGA-NPs carrying single peptide pool were prepared for future injections (one injection/mouse, 3 mice). Briefly, 60 mg of PLGA with or without single peptide pool (575μg/pool, 72-82 μg/peptide) was dissolved in 15mL of dichloromethane followed by ultrasonic dispersion for 30s at 40% amplitude to get the

bioRxiv preprint doi: https://doi.org/10.1101/2021.04.01.438020; this version posted May 24, 2021. The copyright holder for this preprint (which was not certified by peer review) is the author/funder. All rights reserved. No reuse allowed without permission.

primary emulsion. Then, the primary emulsion was added into 150mL of 1% polyvinyl alcohol and sonicated for another 90 s to form the secondary emulsion. The resulting emulsion was added into 300mL of 0.5% PVA solution drop by drop with incessant magnetic stir to allow the evaporation of the dichloromethane. Four hours later, the solution was collected and centrifuged at 6,000 rpm for 5 min. The supernatant was harvested and was ultracentrifuged twice at 12,000 rpm for 10 min. The resulting PLGA-NPs were dispersed in deionized water and were further mixed with EDC and NHS solution for 1 h to allow surface activation of –COOH. After washing, the solution was added dropwise in 1% PEI with a magnetic stirrer for 4 hours at RT. Then, PEI-conjugated NPs were then collected and coincubated with single peptide pool (575μg/pool, 72-82 μg/peptide) in sterile PBS overnight at 4°C on a rotator. Finally, the peptides-encapsulated and - surface coupled PLGA-NPs/peptides vaccine was collected and preserved at 4 ℃ for further use.

12. **Preparation of Poly I:C/peptides and R848/peptides vaccines and mice immunization**

At day 0, mice were injected subcutaneously as the primary immunization. After that, booster immunizations were applied at day 7 and 21. At day 28, mice were executed for further study. The amount of each peptide for each inoculation was 10μg/mouse per time point, so, the amount of each peptide pool was 70 or 80μg/mouse/time point. Each mouse was inoculated with four peptide pools per time point. Each peptide pool was inoculated at one injection site (subcutaneously at tail root, back of the neck and around the groin). Twelve female HLA-A2/DR1 transgenic mice were randomly divided into four groups. The immunization groups, vaccines formula and vaccination scheme were described in Table S4.

13. ELISPOT and ICS

bioRxiv preprint doi: https://doi.org/10.1101/2021.04.01.438020; this version posted May 24, 2021. The copyright holder for this preprint (which was not certified by peer review) is the author/funder. All rights reserved. No reuse allowed without permission.

96-well PVDF-membrane microplates (Merck&Millipore) were coated with anti-IFN-γ capture monoclonal antibody (BD) at 4℃ overnight, and were washed and blocked. Spleen cells (2×10^5/100μL) of primed mice were added into each well, together with single peptide pool (2μg/well for each peptide), PHA (10μg/mL as positive controls), irrelevant epitope peptides (HLA-A2-restricted $AFP_{158-166}$ and A24-restricted $AFP_{424-432}$, 2μg/well for each peptide as no-specific control) or no peptide (negative control). After incubation for 20 h at 37 ℃ and 5% CO_2, the plates were washed and then incubated with biotinylated anti-IFN-γ detecting antibody (BD) for 2h at RT. The plates were washed and then incubated with the streptavidin-conjugated HRP (BD) for 1h at RT. After washing the plates, AEC solution (BD) was used as the color developing agent and the developed spots were imaged and enumerated with professional plate reader.

Additionally, Spleen cells of primed mice were incubated with single peptide pool (20μg/mL for each peptide), PHA (10μg/mL), irrelevant epitope peptides ($AFP_{158-166}$ and $AFP_{424-432}$, 20μg/mL for each peptide) or no peptide for 16 hours in serum-free RPMI-1640 medium in 48-well plate at 37℃ and 5% CO2. After that, BFA/Monensin mixture was added to the cells for another 6-hour culture. Cells were then harvested, washed, blocked with anti-mouse CD16/CD32 for 20 minutes at 4℃ and were stained with FITC-labeled anti-CD3 and PE-labeled anti-CD8 antibodies for 30 min at 4 ℃. After washing, cells were fixed and permeabilized following the protocol and were further incubated with APC-anti-mouse IFN-γ (XMG1.2) (BD) for another 30 min at 4℃ followed by flow cytometry. The frequencies of IFN-γ^+ cells in $CD3^+/CD8^+$ populations were calculated.

14. **ELISA**

bioRxiv preprint doi: https://doi.org/10.1101/2021.04.01.438020; this version posted May 24, 2021. The copyright holder for this preprint (which was not certified by peer review) is the author/funder. All rights reserved. No reuse allowed without permission.

Spleen cells were incubated with single peptide pool (16μg/mL for each peptide) or no peptide (negative control) in 48-well plate for 3 days at 37℃ and 5% CO_2. Then, the supernatants were collected for ELISA. The mouse IFN-γ detection ELISA kit (Dakewe, China) was used to quantify the IFN-γ in supernatants according to manufactor's protocol.

15. Hematoxylin-eosin staining

28 days after primary immunization, the heart, liver, lung and kidney from executed mice were immersed in 4% paraformaldehyde overnight. After that, individual lobes of organs' biopsy material were placed in processing cassettes, dehydrated through a serial alcohol gradient, and embedded in paraffin wax blocks. 5-μm-thick tissue sections were dewaxed in xylene, rehydrated through decreasing concentrations of ethanol, and washed in PBS. Then hematoxylin and eosin staining was carried out routinely.

Acknowledgement

This work was supported by National Nature Science Foundation of China (82041006) and COVID-19 Emergency Research Fund of Zhejiang University of China (2020XGZX021). The sponsors had no role in study design, data collection and analysis, preparation of the manuscript, or decision to submit the article for publication.

Author Contributions

C.S., Y.H. and G.Z. designed and supervised the research. X.J. and Y.D. performed the main experiments of this study. S.S. performed the transgenic mice experiments. X.W. and Z.Z. assisted in the PBMC preparation, cell cultures and flow cytometry and consequent data

bioRxiv preprint doi: https://doi.org/10.1101/2021.04.01.438020; this version posted May 24, 2021. The copyright holder for this preprint (which was not certified by peer review) is the author/funder. All rights reserved. No reuse allowed without permission.

646 analysis. X.L. performed the HLA genotyping and assisted in the generation of HMy2.CIR
647 cell lines expressing indicated HLA-A allotypes. A.S and Y.W assisted in the preparation of
648 peptide cocktail vaccines and mice immunizations. M.L. and X.C collected healthy donors'
649 blood samples and separated the PBMCs. J.L. and B.L. assisted in the on-silicon prediction of
650 epitopes and affinity analysis with HLA-A molecules. C.S. and X.J. wrote the manuscript
651 with discussions from all authors. Y.H., J. Z and H.Q. analyzed and organized the whole data
652 and assisted in the revision of manuscript.
653

654 **Conflict of Interests**

655 The authors declare no competing financial interests related to this study.
656

657 **References**

658 1. Reche, P. A. Potential Cross-Reactive Immunity to SARS-CoV-2 From Common Human
659 Pathogens and Vaccines. Front. Immunol. **11**, 586984 (2020).
660 2. Chen, Z. et al. T and B cell Epitope analysis of SARS-CoV-2 S protein based on
661 immunoinformatics and experimental research. J. Cell. Mol. Med. **25**, 1274-1289 (2021).
662 3. Jeyanathan, M. et al. Immunological considerations for COVID-19 vaccine strategies.
663 Nat. Rev. Immunol. **20**, 615-632(2020).
664 4. Krammer, F. SARS-CoV-2 vaccines in development. Nature **586**, 516-527 (2020).
665 5. Addetia, A. et al. Neutralizing Antibodies Correlate with Protection from SARS-CoV-2 in
666 Humans during a Fishery Vessel Outbreak with a High Attack Rate. J. Clin. Microbiol. **58**,
667 e02107-02120 (2020).

bioRxiv preprint doi: https://doi.org/10.1101/2021.04.01.438020; this version posted May 24, 2021. The copyright holder for this preprint (which was not certified by peer review) is the author/funder. All rights reserved. No reuse allowed without permission.

668 6. Long, Q. X. et al. Clinical and immunological assessment of asymptomatic SARS-CoV-2
669 infections. Nat. Med. **26**, 1200-1204 (2020).
670 7. Schmidt, M. E. et al. The CD8 T Cell Response to Respiratory Virus Infections. Front.
671 Immunol. **9**, 678 (2018).
672 8. Braun, J. et al. SARS-CoV-2-reactive T cells in healthy donors and patients with
673 COVID-19. Nature **587**, 270-274 (2020).
674 9. Grifoni, A. et al. Targets of T Cell Responses to SARS-CoV-2 Coronavirus in Humans
675 with COVID-19 Disease and Unexposed Individuals. Cell **181**, 1489-1501 (2020).
676 10. Le, B. N. et al. SARS-CoV-2-specific T cell immunity in cases of COVID-19 and SARS,
677 and uninfected controls. Nature **584**, 457-462 (2020).
678 11. Peng, Y. et al. Broad and strong memory CD4(+) and CD8(+) T cells induced by
679 SARS-CoV-2 in UK convalescent individuals following COVID-19. Nat. Immunol. **21**,
680 1336-1345 (2020).
681 12. Sekine, T. et al. Robust T Cell Immunity in Convalescent Individuals with Asymptomatic
682 or Mild COVID-19. Cell **183**, 158-168 (2020).
683 13. Xu, Z. et al. Pathological findings of COVID-19 associated with acute respiratory distress
684 syndrome. The. Lancet. Respiratory. Medicine. **8**, 420-422 (2020).
685 14. Wang, F. et al. Characteristics of Peripheral Lymphocyte Subset Alteration in COVID-19
686 Pneumonia. J. Infect. Dis. **221**, 1762-1769 (2020).
687 15. Jiang, Y. et al. COVID-19 pneumonia: CD8(+) T and NK cells are decreased in number
688 but compensatory increased in cytotoxic potential. Clin. Immunol. **218**, 108516 (2020).
689 16. Rodriguez, L. et al. Systems-Level Immunomonitoring from Acute to Recovery Phase of

bioRxiv preprint doi: https://doi.org/10.1101/2021.04.01.438020; this version posted May 24, 2021. The copyright holder for this preprint (which was not certified by peer review) is the author/funder. All rights reserved. No reuse allowed without permission.

690 Severe COVID-19. Cell. Rep. Med. **1**, 100078 (2020).

691 17. Mathew, D. et al. Deep immune profiling of COVID-19 patients reveals distinct
692 immunotypes with therapeutic implications. Science **369**, 6508 (2020).

693 18. Meckiff, B. J. et al. Imbalance of Regulatory and Cytotoxic SARS-CoV-2-Reactive
694 CD4(+) T Cells in COVID-19. Cell **183**, 1340-1353 (2020).

695 19. Zhang, J. Y. et al. Single-cell landscape of immunological responses in patients with
696 COVID-19. Nat. Immunol. **21**, 1107-1118 (2020).

697 20. Sauer, K. et al. An Effective COVID-19 Vaccine Needs to Engage T Cells. Front.
698 Immunol. **11**, 581807 (2020).

699 21. Zhuang, Z. et al. Mapping and role of T cell response in SARS-CoV-2-infected mice. J.
700 Exp. Med. **218**, e20202187 (2021).

701 22. Anand, R. et al. Computational perspectives revealed prospective vaccine candidates from
702 five structural proteins of novel SARS corona virus 2019 (SARS-CoV-2). PeerJ **8**, e9855
703 (2020).

704 23. Saha, R. et al. Designing a next generation multi-epitope based peptide vaccine candidate
705 against SARS-CoV-2 using computational approaches. 3. Biotech. **11**, 47 (2021).

706 24. Singh, H. et al. Designing spike protein (S-Protein) based multi-epitope peptide vaccine
707 against SARS COVID-19 by immunoinformatics. Heliyon **6**, e05528 (2020).

708 25. Behmard, E. et al. Immunoinformatic design of a COVID-19 subunit vaccine using entire
709 structural immunogenic epitopes of SARS-CoV-2. Sci. Rep. **10**, 20864 (2020).

710 26. Banerjee, S. et al. Immuno-informatics approach for multi-epitope vaccine designing
711 against SARS-CoV-2. bioRxiv

bioRxiv preprint doi: https://doi.org/10.1101/2021.04.01.438020; this version posted May 24, 2021. The copyright holder for this preprint (which was not certified by peer review) is the author/funder. All rights reserved. No reuse allowed without permission.

https://www.biorxiv.org/content/10.1101/2020.07.23.218529v3 (2020).

27. Noorimotlagh, Z. et al. Immune and bioinformatics identification of T cell and B cell epitopes in the protein structure of SARS-CoV-2: A systematic review. Int. Immunopharmacol. **86**, 106738 (2020).

28. Cun, Y. et al. COVID-19 coronavirus vaccine T cell epitope prediction analysis based on distributions of HLA class I loci (HLA-A, -B, -C) across global populations. Hum. Vaccin. Immunother. **17**, 1097-1108 (2021).

29. Ferretti, A. K. et al. Unbiased Screens Show CD8+ T Cells of COVID-19 Patients Recognize Shared Epitopes in SARS-CoV-2 that Largely Reside outside the Spike Protein. Immunity **53**, 1095-1107 (2020).

30. Mateus, J. G. et al. Selective and cross-reactive SARS-CoV-2 T cell epitopes in unexposed humans Science **370**, 89-94 (2020).

31. Prachar, M. et al. Identification and validation of 174 COVID-19 vaccine candidate epitopes reveals low performance of common epitope prediction tools. Sci. Rep. **10**, 20465 (2020).

32. Kared, H. et al. SARS-CoV-2-specific CD8+ T cell responses in convalescent COVID-19 individuals. J. Clin. Invest. **131**, e145476 (2021).

33. Rydyznski, M. C. Antigen-Specific Adaptive Immunity to SARS-CoV-2 in Acute COVID-19 and Associations with Age and Disease Severity. et al. Cell **183**, 996-1012 (2020).

34. Tang, F. et al. Lack of peripheral memory B cell responses in recovered patients with severe acute respiratory syndrome: a six-year follow-up study. J. Immunol. **186**,

bioRxiv preprint doi: https://doi.org/10.1101/2021.04.01.438020; this version posted May 24, 2021. The copyright holder for this preprint (which was not certified by peer review) is the author/funder. All rights reserved. No reuse allowed without permission.

7264-7268 (2011)

35. Channappanavar, R. et al. Virus-specific memory CD8 T cells provide substantial protection from lethal severe acute respiratory syndrome coronavirus infection. J. Virol. **88**, 11034-11044 (2014).

36. Alcazer, V. et al. Neoepitopes-based vaccines: challenges and perspectives. Eur. J. Cancer. **108**, 55-60 (2019).

37. Sahin, U. T. Personalized vaccines for cancer immunotherapy. Science **359**, 1355-1360 (2018).

38. Ott, P. A. et al. An immunogenic personal neoantigen vaccine for patients with melanoma. Nature **547**, 217-221 (2017).

39. Sahin, U. et al. Personalized RNA mutanome vaccines mobilize poly-specific therapeutic immunity against cancer. Nature **547**, 222-226 (2017).

40. Li, F. et al. Rapid tumor regression in an Asian lung cancer patient following personalized neo-epitope peptide vaccination. Oncoimmunology **5**, e1238539 (2016).

41. Wang, B. et al. Identification of an HLA-A*0201-restricted CD8+ T-cell epitope SSp-1 of SARS-CoV spike protein. Blood **104**, 200-206 (2004).

42. Lacey, S. F. et al. Characterization of immunologic properties of a second HLA-A2 epitope from a granule protease in CML patients and HLA-A2 transgenic mice. Blood **118**, 2159-2169 (2011).

43. Takagi, A. et al. Identification of HLA-A*02:01-restricted candidate epitopes derived from the non-structural polyprotein 1a of SARS-CoV-2 that may be natural targets of CD8(+) T cell recognition in vivo. J. Virol. **Dec 2,** 01837-20 (2020).

bioRxiv preprint doi: https://doi.org/10.1101/2021.04.01.438020; this version posted May 24, 2021. The copyright holder for this preprint (which was not certified by peer review) is the author/funder. All rights reserved. No reuse allowed without permission.

44. Weiskopf, D. et al. Phenotype and kinetics of SARS-CoV-2-specific T cells in COVID-19 patients with acute respiratory distress syndrome. Sci. Immunol. **5**, eabd2071 (2020).

45. Tsuboi, A. et al. Enhanced induction of human WT1-specific cytotoxic T lymphocytes with a 9-mer WT1 peptide modified at HLA-A*2402-binding residues. Cancer. Immunol. Immunother. **51**, 614-620 (2002).

Supplementary information is available at Cellular and Molecular Immunology's website.

Figure legends

Figure 1: Reference epitope peptides were tested in the DC-peptide-PBL co-culture system. The HLA-A restricted HCC 1-1, HCC 1-2, HCC 5-3, HCC 5-4, HCC 5-5, HBV 111 and HBV 118 peptides, which have been validated as real-world epitopes previously in-house by using HCC patients' or chronic hepatitis patient's PBMCs and ELISPOT assay, were co-cultured with DC and PBLs from healthy donor's PBMCs for 14 days. As detected by both IFN-γ ICS and CFSE proliferation analyses, the weak positive reference peptides (HCC 1-1 and HCC 1-2, SFUs/2×10^5 PBMCs <10) were defined as negative peptides while other positive reference peptides (SFUs/2×10^5 PBMCs >15) were identified as immunogenic epitope peptides. The frequency of IFN-γ^+ T cells in $CD3^+/CD8^+$ T cell population increased by more than 100% and proliferation percentage of $CD8^+$ T cells in $CD3^+/CD8^+$ T cell population increased by more than 20%, as compared with the no peptide negative control.

Figure 2: Immunogenicity of candidate epitopes was validated by DC-peptide-PBL co-culture experiments. DCs were induced for 7 days from healthy donor's PBMCs, then

bioRxiv preprint doi: https://doi.org/10.1101/2021.04.01.438020; this version posted May 24, 2021. The copyright holder for this preprint (which was not certified by peer review) is the author/funder. All rights reserved. No reuse allowed without permission.

coincubated with candidate epitope peptides and autologous PBLs for 14 days. Cells were harvested and stimulated by corresponding candidate peptides for another 16 hours followed by IFN-γ ICS. In some co-culture wells, the DC and peptides were co-cultured with CFSE-prelabeled PBLs for 14 days, and cells were then harvested to detect the proliferation percentage of $CD8^+$ T cell. (A) Representative flow plots of IFN-γ ICS. The data in horizontal coordinates mean the frequency of IFN-γ^+ T cells in $CD3^+/CD8^+$ T cell population. (B) Representative flow plots of CFSE staining. The data in horizontal coordinates mean the proliferation percentage of $CD8^+$ T cells in $CD3^+/CD8^+$ T cell population.

Figure 3: T cell epitope peptide cocktail vaccines elicited robust $CD8^+$ T cell responses in transgenic mice. 31 positive epitope peptides restricted by HLA-A2 molecule were used to generate peptide cocktail vaccines in three formulations, and followed by three-round immunizations of HLA-A2/DR1 transgenic C57BL/6 mice. Then, splenocytes were collected 7 days after the last booster and *ex vivo* stimulated with distinct peptide pools according to single protein overnight, followed by IFN-γ ELISPOT and IFN-γ ICS. (A) Total IFN-γ SFUs responding to all peptide pools in each mouse. (B) Deconvolution of the total SFUs in each mouse from A into the single SARS-CoV-2 proteins. (C) Total frequency of IFN-γ^+ T cells reacting to all peptide pools in $CD3^+CD8^+$ T cell population in each mouse. (D) Deconvolution of the total frequency in each mouse from C into the single SARS-CoV-2 proteins. Control group: N.S and PLGA-NPs; Vaccine A group: PLGA-NPs/peptides vaccines; Vaccine B group: R848/peptides vaccines; Vaccine C group: poly I: C/peptides vaccines.

Figure 4: IFN-γ ELISPOT responses against the individual peptide pools. Splenocytes from each primed mouse were harvested 7 days after the last booster and *ex vivo* stimulated

bioRxiv preprint doi: https://doi.org/10.1101/2021.04.01.438020; this version posted May 24, 2021. The copyright holder for this preprint (which was not certified by peer review) is the author/funder. All rights reserved. No reuse allowed without permission.

with 8 different peptide pools covering the 31 epitope peptides or with AFP peptides ($AFP_{158-166}$, $AFP_{424-432}$) as irrelevant control, or without peptide as negative control, and followed by IFN-γ ELISPOT.

Figure 5: Flow plots of IFN-γ ICS responding to the individual peptide pools. Splenocytes from each primed mouse were harvested 7 days after the last booster and *ex vivo* stimulated with 5 different peptide pools according to single protein or with AFP peptides ($AFP_{158-166}$, $AFP_{424-432}$) as irrelevant control, or without peptide as negative control, and followed by IFN-γ ICS. The data in left upper quadrant mean the frequencies of IFN-γ^+ T cells in $CD3^+/CD8^+$ cell populations.

Figure 6: T cell epitope peptide cocktail vaccines elicited robust $CD8^+$ T cell responses as detected by IFN-γ ELISA in transgenic mice and by IFN-γ ICS in WT mice. Splenocytes from each primed HLA-A2/DR1 tansgenic C57BL/6 mice were harvested 7 days after the last booster and *ex vivo* stimulated with 5 different peptide pools according to single protein or without peptide for 3 days. Then supernatants were collected and followed by IFN-γ ELISA. (A) Total IFN-γ level responding to all peptide pools in each mouse. (B) Deconvolution of the total IFN-γ level in each mouse from A into the single SARS-CoV-2 proteins. Similarly, wild-types C57BL/6 mice were divided into two groups and were immunized three times with the Poly I:C/peptides vaccines prepared using the 31 validated epitope peptides or normal saline, respectively. Splenocytes were then collected 7 days after the last booster and *ex vivo* stimulated with 5 different peptide pools overnight, followed by IFN-γ ICS. (C) Total frequency of IFN-γ^+ T cells reacting to all peptide pools in $CD3^+CD8^+$ T cell population in each mouse. (D) Deconvolution of the total frequency in each mouse from C into the single

bioRxiv preprint doi: https://doi.org/10.1101/2021.04.01.438020; this version posted May 24, 2021. The copyright holder for this preprint (which was not certified by peer review) is the author/funder. All rights reserved. No reuse allowed without permission.

822 SARS-CoV-2 proteins.

823 **Figure 7: Flow plots of IFN-γ ICS responding to the individual peptide pools after WT**
824 **mice immunizations.** (A) Splenocytes from each primed WT mouse were harvested 7 days
825 after the last booster and *ex vivo* stimulated with 5 different peptide pools according to single
826 protein or with AFP peptides ($AFP_{158-166}$, $AFP_{424-432}$) as irrelevant control, or without peptide
827 as negative control, and followed by IFN-γ ICS. The data in left upper quadrant mean the
828 frequencies of IFN-γ^+ T cells in $CD3^+/CD8^+$ cell populations. (B) 7 of 31 epitopes restricted
829 by HLA-A2 were identified to be cross-presented by H-2K/D^b molecules. Splenocytes from
830 each primed WT mouse were harvested as described and *ex vivo* stimulated with single
831 peptide, or without peptide as negative control, and followed by IFN-γ ICS. The epitopes
832 were identified as immunogenic peptides when the frequency of IFN-γ^+ T cells in $CD3^+/CD8^+$
833 cell population increased by more than 100% compared with the negative control.
834 Representative flow plots of the 7 positive epitopes were shown.

835 **Figure S1: Generation of mature mDC from adherent monocytes.** PBMCs from healthy
836 donors were seeded into culture flask and the monocytes adhered for 2 h as described in the
837 Methods section. After washing out the non-adherent cells in both systems, the cells were
838 cultured for 5 days with 1,000 IU/mL GM-CSF and 500 IU/mL IL-4. Then the immature DCs
839 were matured with 1μg/mL LPS for another 48 hours. Immature DCs and mature DCs were
840 stained for CD1a, CD80, CD83, CD86, HLA-ABC and HLA-DR. The unstained and stained
841 populations in the histograms are shown in grey and black, respectively. (A) Phenotype of
842 immature DCs on day 5. (B) Phenotype of mature DCs on day 7.

843 **Figure S2: 120 epitopes were validated by DC-peptide-PBL co-culture experiments**

bioRxiv preprint doi: https://doi.org/10.1101/2021.04.01.438020; this version posted May 24, 2021. The copyright holder for this preprint (which was not certified by peer review) is the author/funder. All rights reserved. No reuse allowed without permission.

(IFN-γ ICS flow plots). DCs were induced for 7 days from healthy donor's PBMCs, then coincubated with candidate epitope peptides and autologous PBLs for 14 days. Cells were harvested and stimulated by corresponding candidate peptides for another 16 hours followed by IFN-γ ICS. The presented are flow plots for each positive epitope peptide. The data in horizontal coordinates mean the frequency of IFN-γ^+ T cells in $CD3^+/CD8^+$ T cell population.

Figure S3: 120 candidate epitopes were validated by DC-peptide-PBL co-culture experiments (CFSE staining flow plots). DCs were coincubated with candidate epitope peptides and CFSE-prelabeled PBLs for 14 days. Cells were then analyzed by flow cytometry. The presented are flow plots for each positive epitope peptide. The data in horizontal coordinates mean the proliferation percentage of $CD8^+$ T cells in $CD3^+/CD8^+$ T cell population.

Figure S4: Eight kinds of HMy2.CIR cell lines expressing one indicated HLA-A allotype. The transfected HMy2.CIR cell lines expressing HLA-A2402, A0203, A0201, A0206, A1101, A3303, A0101, or A3001 were generated, respectively, and then sorted by flow cytometry followed by pure culture and sequencing analyses. The purity of CIR-A2402 cells was 94.1% after being sorted with FITC-anti-A24 staining. The purity of CIR-A0203 cell was 84.3% after being sorted with PE-anti-HLA-ABC (W6/32) or PE-anti-HLA-A2.1 staining. The purities of CIR-A0201/0206/1101/3303/0101/3001 were all more than 80% after being sorted with PE-anti-HLA-ABC staining.

Figure S5: Binding affinity of 120 validated epitopes with HLA-A allotypes as defined by HLA-A molecule competitive binding experiments. A series of unlabeled epitope peptides of SRAS-CoV-2 were coincubated, at 5μM and 15μM respectively, with fluorescent-labeled

bioRxiv preprint doi: https://doi.org/10.1101/2021.04.01.438020; this version posted May 24, 2021. The copyright holder for this preprint (which was not certified by peer review) is the author/funder. All rights reserved. No reuse allowed without permission.

reference peptides and CIR cell lines expressing the corresponding HLA-A molecules for 24 hours. Then the competitively binding inhibition (%) of the epitope peptide at 5μM and 15μM was calculated by measuring the CIR cells fluorescence strength. Shown are the histograms of two concentrations (5μM and 15μM). Black solid line was the histogram of 5μM test peptide; dotted line was the histogram of 15μM, test peptide; black filled line was the maximal fluorescence (FITC-labeled reference peptide without competitive peptides) while the lightest gray line was the negative control (background fluorescence with 1640 alone).

Figure S6: Affinity of HLA-A2-restricted epitope peptides with HLA-A0201 molecule as detected by T2 cell binding assay. T2 cells were incubated with single peptide of the 31 epitopes, or with CMVpp65$_{495\text{-}503}$ peptide as positive control, OVA$_{257\text{-}264}$ peptide as negative control, or no peptide and β2-m for 16 hours, then followed by PE-labeled anti-HLA-A2.1 antibody staining to test the up-regulation of HLA-A0201 molecules onto T2 cells. The fluorescence index (FI) was calculated with flow cytometry.

Figure S7: The peptide cocktail vaccines have no visible toxicity on the organs. Seven days after the last booster, all mice were executed. Heart, liver, lung and kidney were taken out, immersed and were finally stained with Hematoxylin-Eosin. No obvious pathological damage was found in all organs in all groups. The representative HE staining of heart, liver, lung and kidney in each mouse from four groups were exhibited in (A), (B), (C) and (D), respectively.

bioRxiv preprint doi: https://doi.org/10.1101/2021.04.01.438020; this version posted May 24, 2021. The copyright holder for this preprint (which was not certified by peer review) is the author/funder. All rights reserved. No reuse allowed without permission.

889 Table 1: 120 SARS-CoV-2 T cell epitopes validated by DC-peptide-PBL co-stimulation
890 experiments.

Epitope	On-silicon HLA-A restriction	Blood donor 1			Blood donor 2			Blood donor 3		
		A allele	Method	Enhance%	A allele	Method	Enhance%	A allele	Method	Enhance%
A1	0201, 0207, 0206, 2402	0201/6843	CFSE	24.4%	3101/0207	IFN-γ	130.0%	1101/0201	IFN-γ	120.7%
A3	0201, 0203, 1101, 1102	0201/2402	IFN-γ	314.2%						
A4	0201, 0207, 0203	0201/3303	IFN-γ	116.2%	6801/3303	IFN-γ	436.6%	2402/0207	IFN-γ	137.3%
A5	0201, 0203	0201/3303	IFN-γ	589.2%	0201/3001	IFN-γ	650.2%	6801/3303	IFN-γ	728.8%
A6	0207, 0206	0206/0207	IFN-γ	198.5%	1101/0206	IFN-γ	263.0%			
A7	0207	0206/0207	IFN-γ	253.8%						
A9	0206	0206/1101	IFN-γ	163.2%	0206/0203	IFN-γ	131.7%	1101/0206	IFN-γ	666.0%
A10	0203	0203/3101	IFN-γ	109.1%						
A12	1101, 1102, 3303	1101/3001	CFSE	22.1%	0201/1101	IFN-γ	158.5%	3303/1101	IFN-γ	263.0%
A16	1101, 3303	0201/1101	CFSE	40.8%						
A18	1102, 3303, 3001	1101/3101	IFN-γ	119.1%						
A19	1102	1101/3101	IFN-γ	102.9%	1101/2402	CFSE	22.3%			
A20	2402	2402/2601	IFN-γ	543.9%	2402/2402	IFN-γ	146.1%			
A21	2402	2402/2601	IFN-γ	1154.4%	2402/2402	IFN-γ	153.2%			
A22	2402	2402/2601	IFN-γ	378.9%						
A23	2402	2402/2601	IFN-γ	303.5%	2402/2402	IFN-γ	135.5%			
A25	3001	1101/3001	CFSE	129.2%						
A26	3001	1101/3001	CFSE	39.5%	1101/3001	IFN-γ	291.0%			
B1	0201, 0206, 0203	0201/3303	IFN-γ	110.8%	0201/3001	IFN-γ	222.9%	6801/3303	IFN-γ	398.0%
B2	0201, 0206, 0203, 0207	0201/0101	IFN-γ	128.1%						
B3	0201, 0207, 0206	0201/3001	IFN-γ	407.3%						
B4	0201, 0206	0201/3001	IFN-γ	216.6%						
B6	0201, 0207, 0203	0203/0207	IFN-γ	242.1%	0201/1101	CFSE	35.7%	2402/0207	IFN-γ	164.8%
B10	0207	0207/0206	IFN-γ	888.7%	3101/0207	IFN-γ	120.0%	2402/0207	IFN-γ	123.8%
B11	0206	0206/1101	IFN-γ	154.5%	0206/3201	CFSE	25.8%	1101/0206	IFN-γ	307.0%
B12	0206	1101/0206	CFSE	22.5%	1101/0206	IFN-γ	104.0%			
B15	0203	0203/3101	IFN-γ	416.5%						

bioRxiv preprint doi: https://doi.org/10.1101/2021.04.01.438020; this version posted May 24, 2021. The copyright holder for this preprint (which was not certified by peer review) is the author/funder. All rights reserved. No reuse allowed without permission.

B16	0203	0203/3001	CFSE	24.7%						
B17	0203	0203/3101	IFN-γ	122.7%						
B18	1101, 1102	1101/3001	CFSE	79.0%						
B20	1101, 1102, 3303	0201/1101	CFSE	33.4%						
B21	1101, 1102	0201/1101	CFSE	55.4%						
B23	1101, 1102, 3303	3303/1101	IFN-γ	431.5%						
B26	2402	2402/2402	IFN-γ	214.5%	2402/2601	IFN-γ	277.2%			
B28	2402	2402/3303	IFN-γ	214.5%						
B29	2402	2402/3303	IFN-γ	500.0%	2402/2402	IFN-γ	341.8%	6801/3303	IFN-γ	142.5%
B30	2402	2402/3303	IFN-γ	362.7%						
B31	2402	2402/2402	IFN-γ	129/0%	2402/2402	IFN-γ	139.0%			
B34	3303	3303/3001	IFN-γ	102.1%						
B35	3303	3303/1101	IFN-γ	148.2%						
B36	3001	1101/3001	CFSE	54.9%	1101/3001	IFN-γ	374.0%			
B37	3001	1101/3001	CFSE	34.9%	3001/2402	IFN-γ	110.5%	1101/3001	IFN-γ	191.0%
B38	3001	2402/3001	IFN-γ	186.8%						
B40	3001	1101/3001	IFN-γ	140.0%						
B41	3001	1101/3001	IFN-γ	425.0%						
C1	0201, 0206, 0203	0201/1101	CFSE	30.0%						
C3	0201, 0206, 0203	0201/2402	IFN-γ	270.9%						
C10	0206	0206/1101	CFSE	25.9%						
C12	0206	0206/3201	CFSE	20.8%						
C16	0206	0206/1101	IFN-γ	187.7%						
C17	0203	0203/3101	IFN-γ	157.4%						
C27	1101	1101/1101	CFSE	40.1%						
C35	2402	2402/2601	IFN-γ	144.0%						
C45	3303	1101/3303	IFN-γ	181.1%						
C46	3303	1101/3303	IFN-γ	100.0%						
C47	3303	1101/0101	IFN-γ	223.8%						
C49	1102	0201/1101	IFN-γ	1663.3%						
D2	0201, 0206, 0203	0201/1101	IFN-γ	122.3%						
D5	0207, 0206, 1102	0206/1102	IFN-γ	479.2%						
D6	0201, 0207	0201/2402	CFSE	105.5%	0201/0101	IFN-γ	106.9%			
D12	0201, 0207, 0206	0201/0201	CFSE	23.4%						
D13	0201, 0203	0201/2402	IFN-γ	1001.3%						

bioRxiv preprint doi: https://doi.org/10.1101/2021.04.01.438020; this version posted May 24, 2021. The copyright holder for this preprint (which was not certified by peer review) is the author/funder. All rights reserved. No reuse allowed without permission.

D17	0207, 0203	0206/0207	IFN-γ	112.3%						
D26	0206	0201/0207	CFSE	29.9%						
D30	0203	0203/0206	CFSE	34.6%	0203/0207	IFN-γ	145.3%			
D31	0203	0203/0206	CFSE	33.5%						
D32	0203	0203/0206	CFSE	33.3%						
D33	0203, 0206	0203/0206	CFSE	28.0%						
D34	1101/1102	1101/0101	IFN-γ	117.2%						
D38	1101, 1102	1101/0101	IFN-γ	105.9%						
D40	1101, 1102, 3001	1101/3303	IFN-γ	100.0%						
D41	1101	1101/0101	IFN-γ	268.0%						
D42	1101, 0206, 0201	1101/0101	IFN-γ	128.4%	1101/1101	CFSE	47.6%			
D46	1102	0201/1101	IFN-γ	458.6%						
D47	1102	0201/1101	IFN-γ	179.9%						
D48	1102, 3303	0201/1101	IFN-γ	166.9%	3303/1101	IFN-γ	117.8%			
D50	1102	0201/1101	IFN-γ	242.0%						
D52	2402	2402/3001	IFN-γ	241.7%						
D53	2402, 3303	2402/3001	IFN-γ	460.8%	3303/1101	IFN-γ	275.5%			
D55	2402	2402/0207	IFN-γ	110.2%						
D56	2402	2402/2601	IFN-γ	266.9%						
D62	2402	2402/3001	IFN-γ	182.4%						
D64	2402	0201/2402	IFN-γ	144.9%						
D65	3001	0101/3001	CFSE	20.8%						
D71	3001	0301/3001	IFN-γ	132.9%						
D72	3001, 1102, 0201, 0207	3303/1101	IFN-γ	157.7%						
D76	3303	1101/0101	IFN-γ	346.7%						
D77	3303, 1102	3303/1101	IFN-γ	109.5%	3303/0203	IFN-γ	102.9%			
D78	3303, 0203, 0206	3303/1101	IFN-γ	101.4%						
D79	3303, 1101, 0207, 2402	3303/1101	IFN-γ	175.8%						
D80	3303, 1102, 0201, 0207	3303/1101	IFN-γ	148.2%						
D81	3303, 1102, 0203	3303/1101	IFN-γ	149.6%						
D82	3303, 1102	3303/1101	IFN-γ	101.7%						
R4	0201	0201/1101	IFN-γ	107.8%	0201/3201	CFSE	47.3%			

bioRxiv preprint doi: https://doi.org/10.1101/2021.04.01.438020; this version posted May 24, 2021. The copyright holder for this preprint (which was not certified by peer review) is the author/funder. All rights reserved. No reuse allowed without permission.

R5	0201, 0203	0201/3201	CFSE	107.8%	0201/0101	IFN-γ	117.5%			
R6	0201, 0207, 0206, 0203	0201/3201	CFSE	49.3%						
R8	0201	0201/0101	IFN-γ	113.2%						
R9	0201, 0206, 0203	0201/0101	IFN-γ	107.0%						
R10	0201	0201/2402	IFN-γ	104.3%						
R11	0201	0201/3001	IFN-γ	203.6%	0201/1101	IFN-γ	104.4%			
R12	0201	0201/3001	IFN-γ	147.0%	0201/0101	IFN-γ	188.6%			
R13	0201	0201/3001	IFN-γ	147.0%	0201/1101	IFN-γ	126.9%			
R14	0201, 0203	0201/0101	IFN-γ	133.3%						
R15	0201	0201/2402	IFN-γ	218.4%						
R17	0207	0207/0206	IFN-γ	103.0%						
R23	0206	2402/0207	IFN-γ	109.4%						
R24	0203	0203/0206	CFSE	60.8%						
R30	1101	1101/3001	CFSE	110.2%	0201/1101	CFSE	38.7%			
R32	1101/1102	0201/1101	CFSE	29.3%						
R34	1101, 3001	0201/1101	CFSE	20.0%	1101/3101	IFN-γ	122.1%			
R35	1101, 1102	1101/3101	CFSE	24.9%						
R38	1101, 3303	0201/1101	CFSE	50.2%						
R39	1101, 1102, 3001	0201/1101	CFSE	54.3%						
R40	1101, 3001	0201/1101	CFSE	39.7%	0201/1101	CFSE	19.5%			
R41	1101, 3303	0201/1101	CFSE	53.3%						
R42	1101	0201/1101	CFSE	21.0%						
R43	1101, 3303	1101/3001	CFSE	41.9%	0201/1101	CFSE	34.5%			
R44	1101, 1102	0201/1101	CFSE	37.6%	0201/1101	CFSE	24.8%			
R47	2402	2402/3303	IFN-γ	339.8%						
R48	2402	2402/3303	IFN-γ	309.6%						

Note 1: **CFSE:** After DC-peptide-CFSE-prelabeled PBLs co-cultures, the proliferation percentage of $CD8^+$ T cells in $CD3^+/CD8^+$ population was analyzed according to the reduction of CFSE-staining brightness. **IFN-γ:** After DC-peptide-PBLs co-cultures, the frequency of IFN-$\gamma^+/CD8^+$ T cells in $CD3^+/CD8^+$ population was analyzed by flow cytometry. **Enhance%:** The increased percentage when the frequency of IFN-$\gamma^+/CD8^+$ T cells or proliferation percentage of $CD8^+$ T cells in the DC-peptide-PBL co-culture wells was compared with that in the DC-PBL co-culture well without peptide. Note 2: The previously reported epitopes include C1, C35, C49, D34, D46, D47, D48, D52, D53 and R32.

bioRxiv preprint doi: https://doi.org/10.1101/2021.04.01.438020; this version posted May 24, 2021. The copyright holder for this preprint (which was not certified by peer review) is the author/funder. All rights reserved. No reuse allowed without permission.

898 Table 2: Affinity of SARS-CoV-2 $CD8^+$ T cell epitopes with HLA-A allotypes as detected by

899 HLA-A competitive binding experiments using HMy2.CIR cell lines.

HLA-A	Epitope	Affinity	5μM Competitive inhibition%	15μM Competitive inhibition%	Epitope	Affinity	5μM Competitive inhibition%	15μM Competitive inhibition%
A*0201	R12	high	91.70%	91.10%	R6	low/no	13.40%	23.70%
	R8	high	85.50%	89.90%	D5	low/no	10.00%	37.80%
	B1	high	80%	88.20%	A5	low/no	9.40%	6.20%
	R10	high	75.80%	92.80%	R13	low/no	8.66%	28.90%
	R15	high	70.80%	93.80%	D80	low/no	6.38%	5.25%
	B3	high	66.10%	74.40%	D42	low/no	5.93%	6.72%
	R9	high	64.80%	89.50%	D72	low/no	5.93%	6.38%
	R5	high	58.70%	89.10%	A4	low/no	4.80%	4.00%
	R11	inter	47.80%	86.40%	R14	low/no	4.50%	13.30%
	B2	inter	42.10%	83.70%	A1	low/no	3.30%	2.90%
	R4	inter	40.40%	78.30%	A3	low/no	1.90%	1.40%
	B6	inter	33.00%	65.90%	D13	low/no	0.70%	1.20%
	D2	inter	24.50%	55.00%	C1	low/no	0	10.30%
	D12	low/no	20.10%	32.60%	C3	low/no	0	7.10%
	B4	low/no	16.70%	20.70%	D6	low/no	0	2.10%
A*1101	D38	high	80.70%	87.70%	D48	low/no	34.38%	48.05%
	D41	high	80.38%	89.72%	D50	low/no	32.38%	43.38%
	R43	high	79.50%	89.20%	B23	low/no	32.30%	41.00%
	R32	high	73.90%	89.40%	R41	low/no	31.90%	46.20%
	R30	high	72.60%	84.90%	B18	low/no	21.55%	34.38%
	D34	high	67.70%	84.70%	D82	low/no	20.72%	38.22%
	B20	high	61.88%	55.88%	A16	low/no	18.38%	19.22%
	D72	high	58.05%	76.05%	D77	low/no	15.72%	29.38%
	D40	high	56.70%	82.60%	D42	low/no	14.70%	47.80%
	D47	high	53.38%	67.72%	A12	low/no	14.38%	15.00%
	R42	high	50.20%	75.20%	R38	low/no	12.10%	47.10%
	R44	inter	47.60%	81.4	B21	low/no	10.55%	29.38%
	C49	inter	47.38%	74.22%	D79	low/no	10.22%	25.22%
	D81	inter	0.4238	52.22%	R34	low/no	10.00%	25.90%
	D46	inter	34.38%	52.22%	D80	low/no	4.22%	5.55%
	R40	inter	30.70%	67.10%	A19	low/no	0.20%	2.60%
	C27	inter	28.00%	54.40%	A18	low/no	0	4.00%
	R39	inter	23.70%	53.60%				
	R35	inter	22.50%	52.30%				
A*3303	D80	high	86.40%	97.40%	B23	low/no	21.26%	34.07%
	D76	high	75.40%	94.20%	B21	low/no	20.36%	46.43%

bioRxiv preprint doi: https://doi.org/10.1101/2021.04.01.438020; this version posted May 24, 2021. The copyright holder for this preprint (which was not certified by peer review) is the author/funder. All rights reserved. No reuse allowed without permission.

	R34	high	72.50%	91.00%	R38	low/no	18.79%	42.61%
	D77	high	64.20%	81.80%	D53	low/no	14.94%	35.87%
	R43	high	60.81%	65.75%	D48	low/no	13.39%	43.28%
	D82	high	49.40%	75.90%	C46	low/no	10.90%	42.80%
	B34	inter	41.26%	54.29%	A18	low/no	8.90%	11.15%
	D79	inter	33.10%	62.70%	B35	low/no	8.10%	41.40%
	D81	inter	16.00%	74.00%	B20	low/no	7.10%	14.74%
	C47	inter	9.90%	60.20%	A12	low/no	6.65%	0.00%
	R41	inter	8.00%	51.15%	D78	low/no	3.30%	20.30%
	A16	low/no	42.61%	46.43%	C45	low/no	0.00%	29.10%
A*0203	D30	high	82.80%	91.80%	B16	low/no	38.10%	38.00%
	R24	high	61.30%	78.80%	D17	low/no	21.83%	43.31%
	B17	high	57.00%	70.50%	C3	low/no	11.44%	28.39%
	B15	high	50%	54.00%	B6	low/no	6.43%	46.41%
	D5	high	70.87%	83.76%	R6	low/no	5.84%	8.10%
	R5	high	60.37%	81.49%	A4	low/no	4.64%	8.94%
	R9	high	59.30%	81.61%	A5	low/no	5.24%	11.09%
	D2	high	53.45%	55.36%	D81	low/no	4.64%	6.79%
	B2	high	51.90%	68.84%	D78	low/no	3.93%	3.21%
	D33	inter	42.30%	81.20%	D31	low/no	0	14.80%
	B1	inter	37.82%	57.74%	A10	low/no	0	0
	R14	inter	37.10%	65.74%	D32	low/no	0	0
	D13	inter	25.29%	55.48%				
	C17	inter	21.70%	51.30%				
	C1	inter	20.39%	54.54%				
A*0206	D26	high	52.30%	68.10%	C10	low/no	17.08%	31.68%
	R23	inter	39.30%	50.10%	D12	low/no	17.08%	29.07%
	B3	inter	42.63%	57.11%	A1	low/no	16.30%	16.95%
	D2	inter	41.72%	63.49%	C1	low/no	15.91%	21.77%
	B1	inter	41.20%	60.37%	A6	low/no	15.51%	13.30%
	B2	inter	37.29%	54.89%	R6	low/no	14.73%	18.64%
	D33	inter	35.72%	68.19%	C16	low/no	12.65%	13.69%
	R9	inter	30.12%	73.53%	C3	low/no	12.65%	13.30%
	C12	low/no	19.43%	36.25%	D42	low/no	9.26%	12.78%
	B4	low/no	18.77%	14.34%	D78	low/no	8.47%	8.34%
	B11	low/no	18.30%	43.40%	A9	low/no	0	10.20%
	B12	low/no	17.00%	32.60%				
A*2402	B30	high	88.65%	91.49%	B28	low/no	18.00%	28.20%
	R47	high	88.50%	88.70%	A22	low/no	10.70%	29.30%
	B26	high	83.60%	82.60%	D52	low/no	6.25%	24.78%
	B31	high	81.10%	86.30%	A1	low/no	5.60%	7.20%
	D55	high	73.07%	78.50%	A20	low/no	5.30%	21.30%
	B29	high	70.10%	74.90%	C35	low/no	2.80%	10.10%

bioRxiv preprint doi: https://doi.org/10.1101/2021.04.01.438020; this version posted May 24, 2021. The copyright holder for this preprint (which was not certified by peer review) is the author/funder. All rights reserved. No reuse allowed without permission.

	D53	high	59.85%	62.21%	A23	low/no	1.20%	1.20%
	R48	inter	40.10%	51.00%	A19	low/no	0.00%	0.00%
	D62	inter	37.53%	75.19%	A21	low/no	0.00%	0.00%
	D64	inter	35.05%	69.41%	D79	low/no	0.00%	0.00%
	D56	low/no	30.21%	45.80%				
A*0207	A7	high	68.52%	69.58%	R6	low/no	35.22%	48.64%
	B2	high	63.58%	64.64%	D72	low/no	32.87%	41.69%
	R17	high	57.11%	62.75%	D80	low/no	20.64%	47.93%
	B6	high	56.40%	60.87%	D79	low/no	18.75%	29.58%
	A6	high	54.99%	62.05%	D17	low/no	16.40%	21.11%
	B3	high	54.99%	63.34%	D5	low/no	11.46%	44.64%
	A1	inter	45.22%	50.16%	B10	low/no	2.40%	0.00%
	D6	low/no	46.40%	48.05%	D12	low/no	0.00%	0.00%
	A4	low/no	36.40%	40.40%				
A*3001	D65	high	75.62%	79.92%	D72	inter	44.70%	62.45%
	D71	high	72.12%	65.13%	R34	inter	31.53%	54.11%
	B40	high	63.52%	72.12%	R40	low/no	38.25%	29.92%
	B41	high	60.30%	60.30%	A26	low/no	37.18%	18.90%
	B36	high	60.03%	73.20%	D40	low/no	36.91%	42.55%
	B37	high	54.11%	60.03%	A25	low/no	20.51%	33.15%
	B38	inter	49.54%	61.91%	A18	low/no	15.94%	35.83%
	R39	inter	46.05%	55.46%				

Note: IC50 is the concentration of unlabeled peptide required to inhibit the binding of labeled reference peptide by 50%, which is calculated from the competitively binding inhibition (%) of the sample at 5μM and 15μM.

Binding affinity of unlabeled peptide with indicated HLA-A molecule is assessed by IC50. IC50<5μM means high binding affinity, between 5-15μM means intermediate binding affinity, more than 15μM means low binding affinity or no binding affinity.

bioRxiv preprint doi: https://doi.org/10.1101/2021.04.01.438020; this version posted May 24, 2021. The copyright holder for this preprint (which was not certified by peer review) is the author/funder. All rights reserved. No reuse allowed without permission.

914 Table 3: HLA-A restrictions of the 120 SARS-CoV-2 epitopes

Epitope	On-silicon prediction	CIR cell lines HLA-A competitive binding assay			No test
		High affinity	Inter affinity	low/no affinity	
A1	A0201,A0207,A0206, A2402		A0207	A0206 >A2402 >A0201	
A3	A0201			A0201	
A4	A0201, A0207, A0203			A0207>A0201 > A0203	
A5	A0201, A0203			A0201> A0203	
A6	A0207, A0206	A0207		A0206	
A7	A0207	A0207			
A9	A0206			A0206	
A10	A0203			A0203	
A12	A1101, A1102, A3303			A1101 > A3303	A1102
A16	A1101, A3303			A3303 > A1101	
A18	A1102, A3303, A3001			A3001>A3303 > A1101	
A19	A1102			A1101	A1102
A20	A2402			A2402	
A21	A2402			A2402	
A22	A2402			A2402	
A23	A2402			A2402	
A25	A3001			A3001	
A26	A3001			A3001	
B1	A0201, A0206, A0203	A0201	A0206 >A0203		
B2	A0201, A0206, A0203, A0207	A0207>A0203	A0201 > A0206		
B3	A0201, A0207, A0206	A0201>A0207	A0206		
B4	A0201, A0206			A0206 >A0201	
B6	A0201, A0207, A0203	A0207	A0201	A0203	
B10	A0207			A0207	
B11	A0206			A0206	
B12	A0206			A0206	
B15	A0203	A0203			
B16	A0203			A0203	
B17	A0203	A0203			
B18	A1101, A1102			A1101	A1102
B20	A1101, A1102, A3303	A1101		A3303	A1102
B21	A1101, A1102			A1101	A1102
B23	A1101, A1102, A3303			A1101 > A3303	A1102
B26	A2402	A2402			
B28	A2402			A2402	
B29	A2402	A2402			
B30	A2402	A2402			

bioRxiv preprint doi: https://doi.org/10.1101/2021.04.01.438020; this version posted May 24, 2021. The copyright holder for this preprint (which was not certified by peer review) is the author/funder. All rights reserved. No reuse allowed without permission.

B31	A2402	A2402			
B34	A3303		A3303		
B35	A3303			A3303	
B36	A3001	A3001			
B37	A3001	A3001			
B38	A3001		A3001		
B40	A3001	A3001			
B41	A3001	A3001			
C1	A0201, A0206, A0203		A0203	A0206 >A0201	
C3	A0201, A0206, A0203			A0206 > A0203 >A0201	
C10	A0206			A0206	
C12	A0206			A0206	
C16	A0206			A0206	
C17	A0203		A0203		
C27	A1101		A1101		
C35	A2402			A2402	
C45	A3303			A3303	
C46	A3303			A3303	
C47	A3303		A3303		
C49	A1102		A1101		A1102
D2	A0201, A0206, A0203	A0203	A0206 >A0201		
D5	A0201, A0207, A0203	A0203		A0207>A0201	
D6	A0201, A0207			A0207>A0201	
D12	A0201, A0207, A0206		A0206	A0201>A0207	
D13	A0201, A0203		A0203	A0201	
D17	A0207, A0203			A0203>A0207	
D26	A0206	A0206			
D30	A0203	A0203			
D31	A0203			A0203	
D32	A0203			A0203	
D33	A0203, A0206		A0203 >A0206		
D34	A1101, A1102	A1101			A1102
D38	A1101, A1102	A1101			A1102
D40	A1101, A1102, A3001	A1101		A3001	A1102
D41	A1101	A1101			
D42	A1101, A0206, A0201			A1101> A0206 > A0201	
D46	A1102		A1101		A1102
D47	A1102	A1101			A1102
D48	A1102, A3303			A1101 > A3303	A1102
D50	A1102			A1101	A1102
D52	A2402			A2402	
D53	A2402, A3303	A2402		A3303	
D55	A2402	A2402			

bioRxiv preprint doi: https://doi.org/10.1101/2021.04.01.438020; this version posted May 24, 2021. The copyright holder for this preprint (which was not certified by peer review) is the author/funder. All rights reserved. No reuse allowed without permission.

D56	A2402			A2402	
D62	A2402		A2402		
D64	A2402		A2402		
D65	A3001	A3001			
D71	A3001	A3001			
D72	A3001,A1102,A0201, A0207	A1101	A3001	A0207>A0201	
D76	A3303	A3303			
D77	A3303, A1102	A3303		A1101	A1102
D78	A3303, A0203, A0206			A0206 >A0203 > A3303	
D79	A3303, A1101, A0207, A2402		A3303	A0207>A1101 > A2402	
D80	A3303,A1102,A0201, A0207	A3303		A0207>A0201 > A1101	A1102
D81	A3303, A1102, A0203		A1101 > A3303	A0203	A1102
D82	A3303, A1102	A3303		A1101	A1102
R4	A0201		A0201		
R5	A0201, A0203	A0203 > A0201			
R6	A0201,A0207,A0206, A0203			A0207>A0206>A0201> A0203	
R8	A0201	A0201			
R9	A0201, A0206, A0203	A0201 > A0203	A0206		
R10	A0201	A0201			
R11	A0201		A0201		
R12	A0201	A0201			
R13	A0201			A0201	
R14	A0201, A0203		A0203	A0201	
R15	A0201	A0201			
R17	A0207	A0207			
R23	A0206		A0206		
R24	A0203	A0203			
R30	A1101	A1101			
R32	A1101, A1102	A1101			A1102
R34	A1101, A3001, A3303	A3303	A3001	A1101	
R35	A1101, A1102		A1101		A1102
R38	A1101, A3303			A3303 > A1101	
R39	A1101, A1102, A3001		A1101		A1102
R40	A1101, A3001		A1101	A3001	
R41	A1101, A3303		A3303	A1101	
R42	A1101	A1101			
R43	A1101, A3303	A1101 > A3303			
R44	A1101, A1102		A1101		A1102
R47	A2402	A2402			

bioRxiv preprint doi: https://doi.org/10.1101/2021.04.01.438020; this version posted May 24, 2021. The copyright holder for this preprint (which was not certified by peer review) is the author/funder. All rights reserved. No reuse allowed without permission.

R48	A2402		A2402		

Note: The HLA-A molecules highlighted in red displayed no affinity with indicated epitopes. " > " means the affinity from high to low.

bioRxiv preprint doi: https://doi.org/10.1101/2021.04.01.438020; this version posted May 24, 2021. The copyright holder for this preprint (which was not certified by peer review) is the author/funder. All rights reserved. No reuse allowed without permission.

Figure 1:

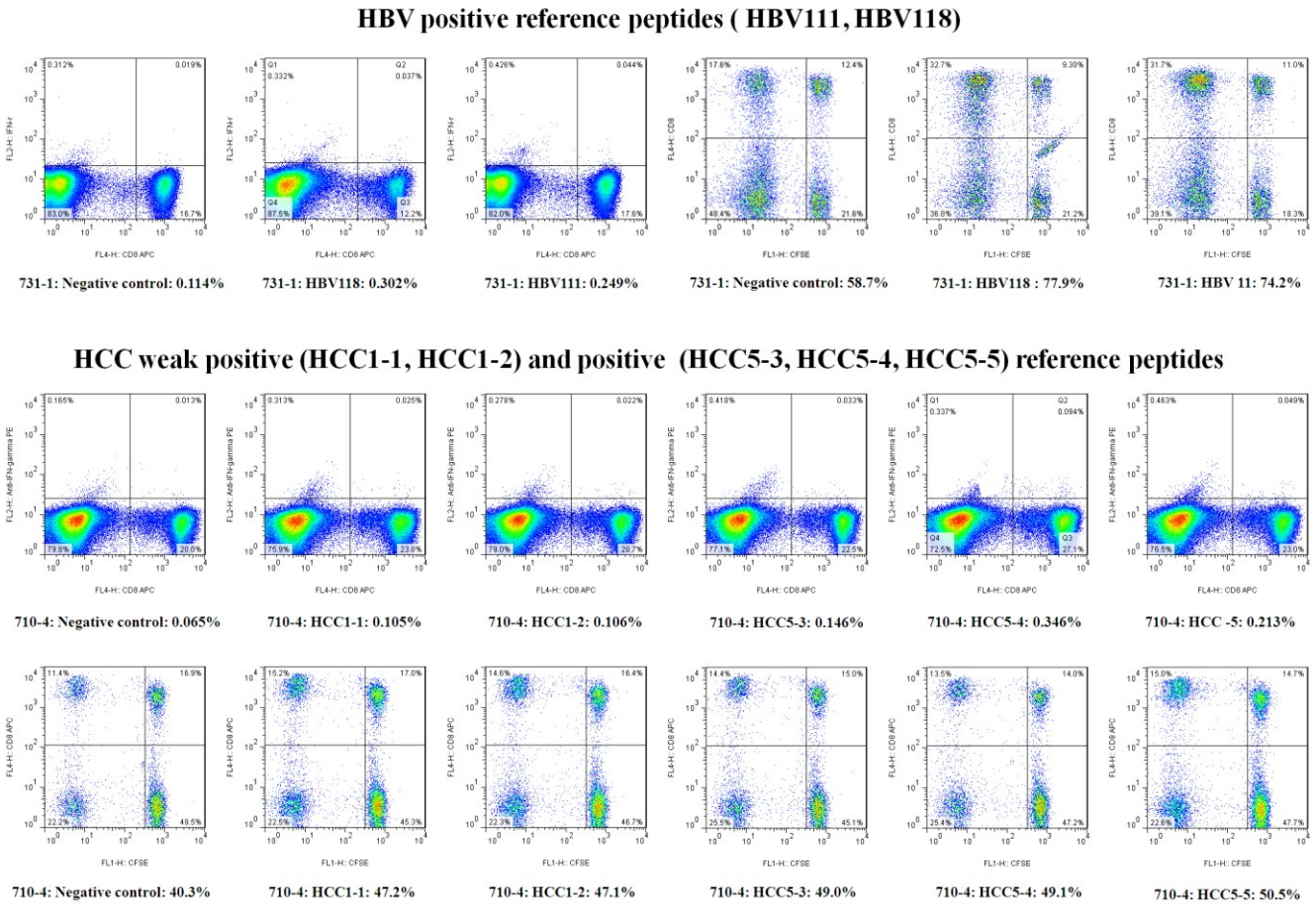

bioRxiv preprint doi: https://doi.org/10.1101/2021.04.01.438020; this version posted May 24, 2021. The copyright holder for this preprint (which was not certified by peer review) is the author/funder. All rights reserved. No reuse allowed without permission.

Figure 2:

A IFN-γ

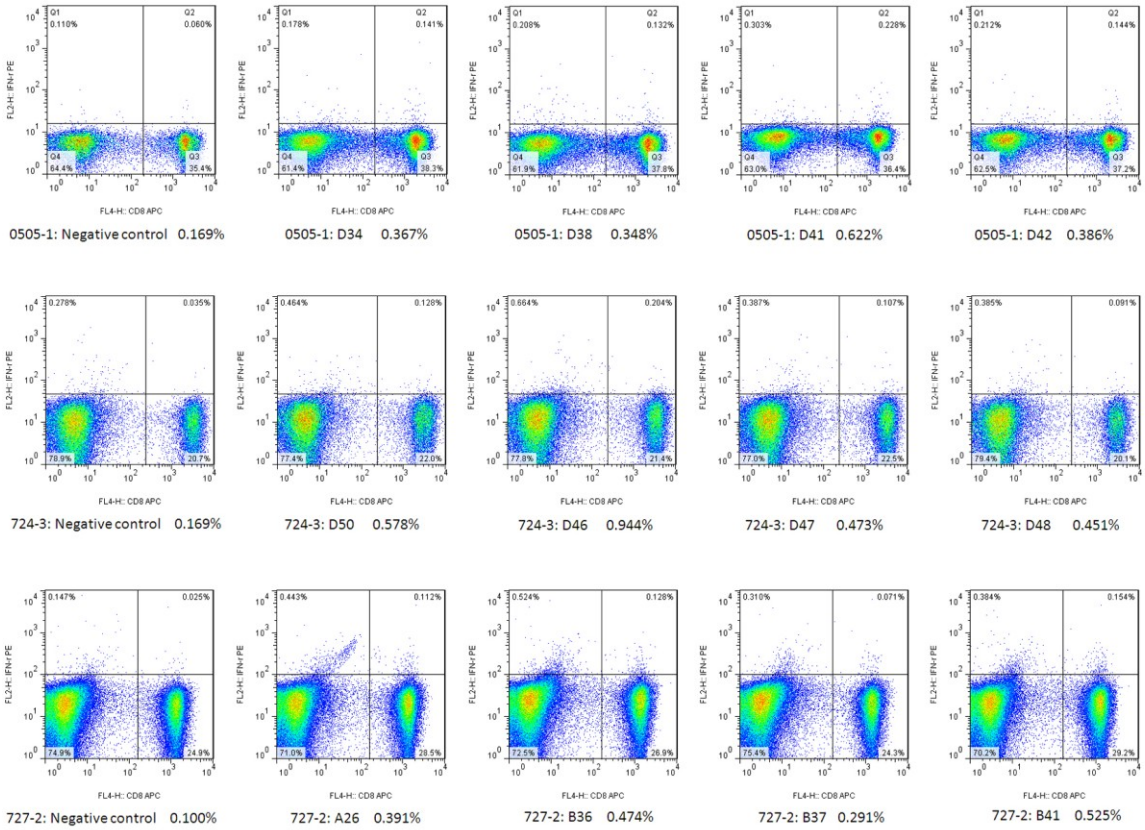

B CFSE

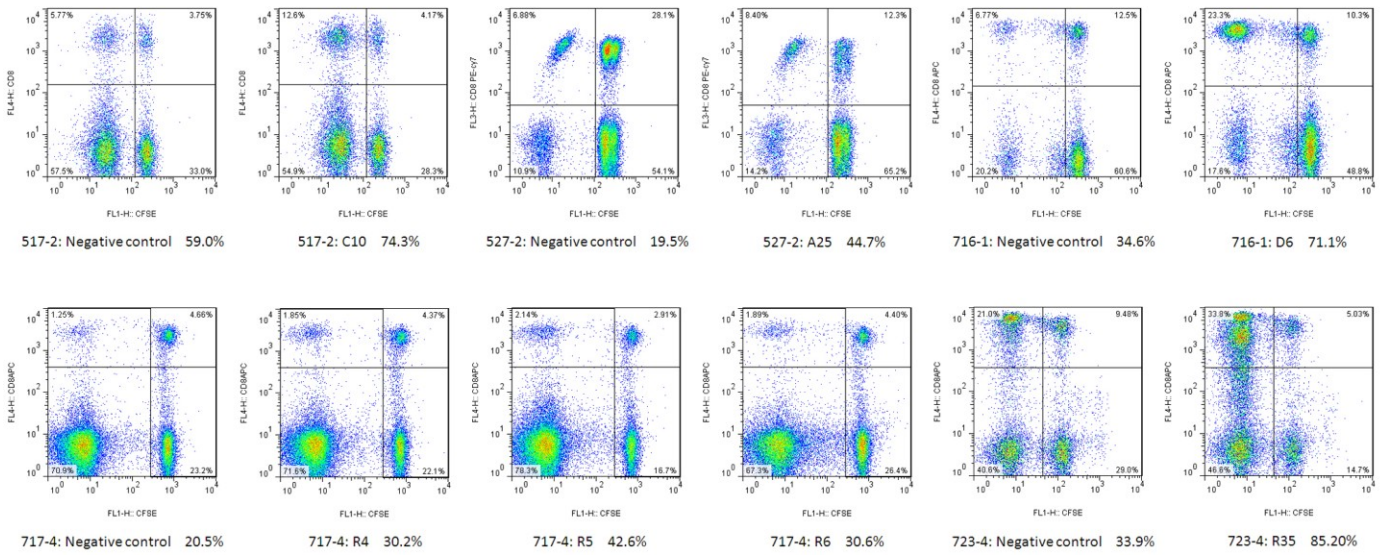

bioRxiv preprint doi: https://doi.org/10.1101/2021.04.01.438020; this version posted May 24, 2021. The copyright holder for this preprint (which was not certified by peer review) is the author/funder. All rights reserved. No reuse allowed without permission.

Figure 3:

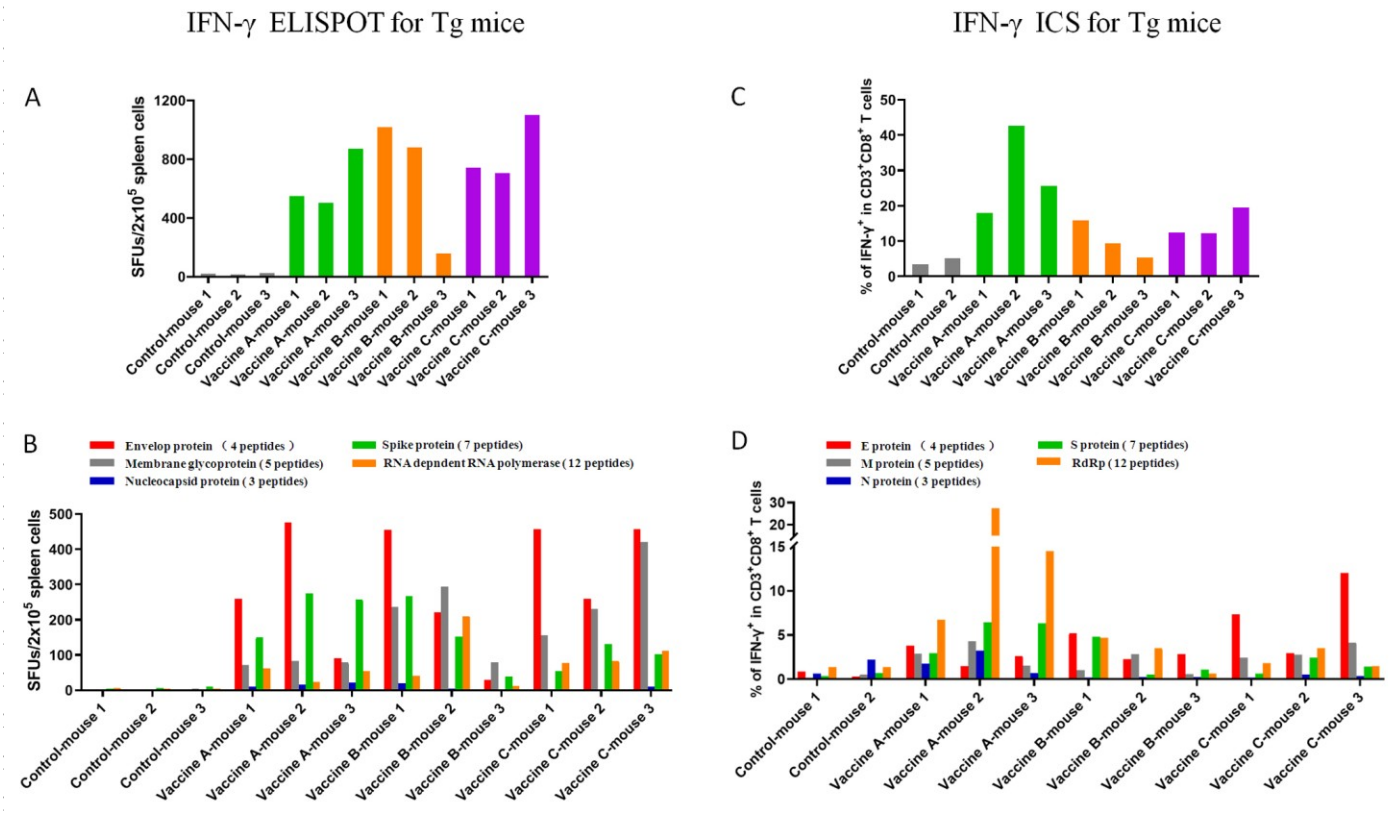

bioRxiv preprint doi: https://doi.org/10.1101/2021.04.01.438020; this version posted May 24, 2021. The copyright holder for this preprint (which was not certified by peer review) is the author/funder. All rights reserved. No reuse allowed without permission.

Figure 4:

bioRxiv preprint doi: https://doi.org/10.1101/2021.04.01.438020; this version posted May 24, 2021. The copyright holder for this preprint (which was not certified by peer review) is the author/funder. All rights reserved. No reuse allowed without permission.

Figure 5:

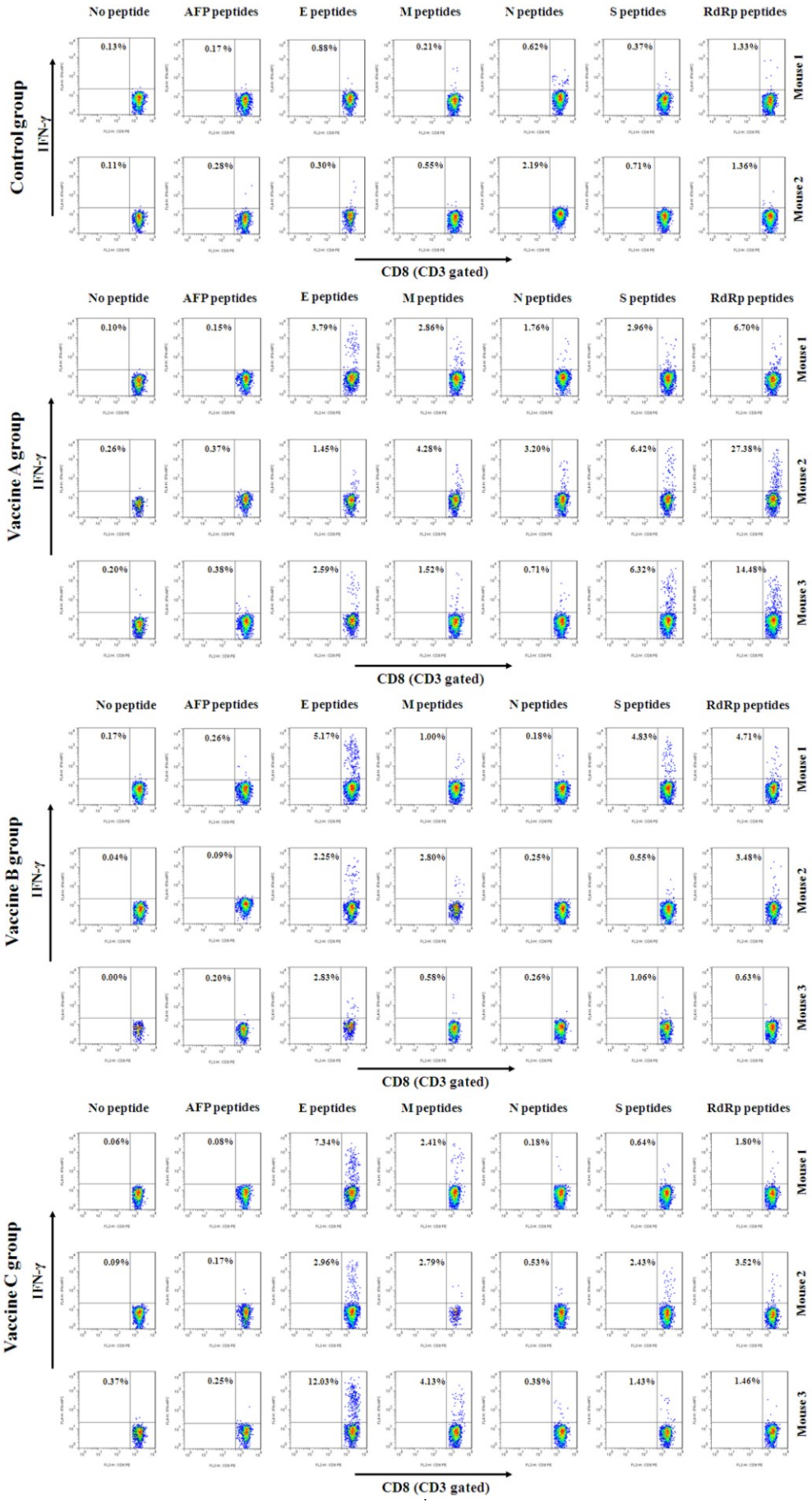

bioRxiv preprint doi: https://doi.org/10.1101/2021.04.01.438020; this version posted May 24, 2021. The copyright holder for this preprint (which was not certified by peer review) is the author/funder. All rights reserved. No reuse allowed without permission.

Figure 6:

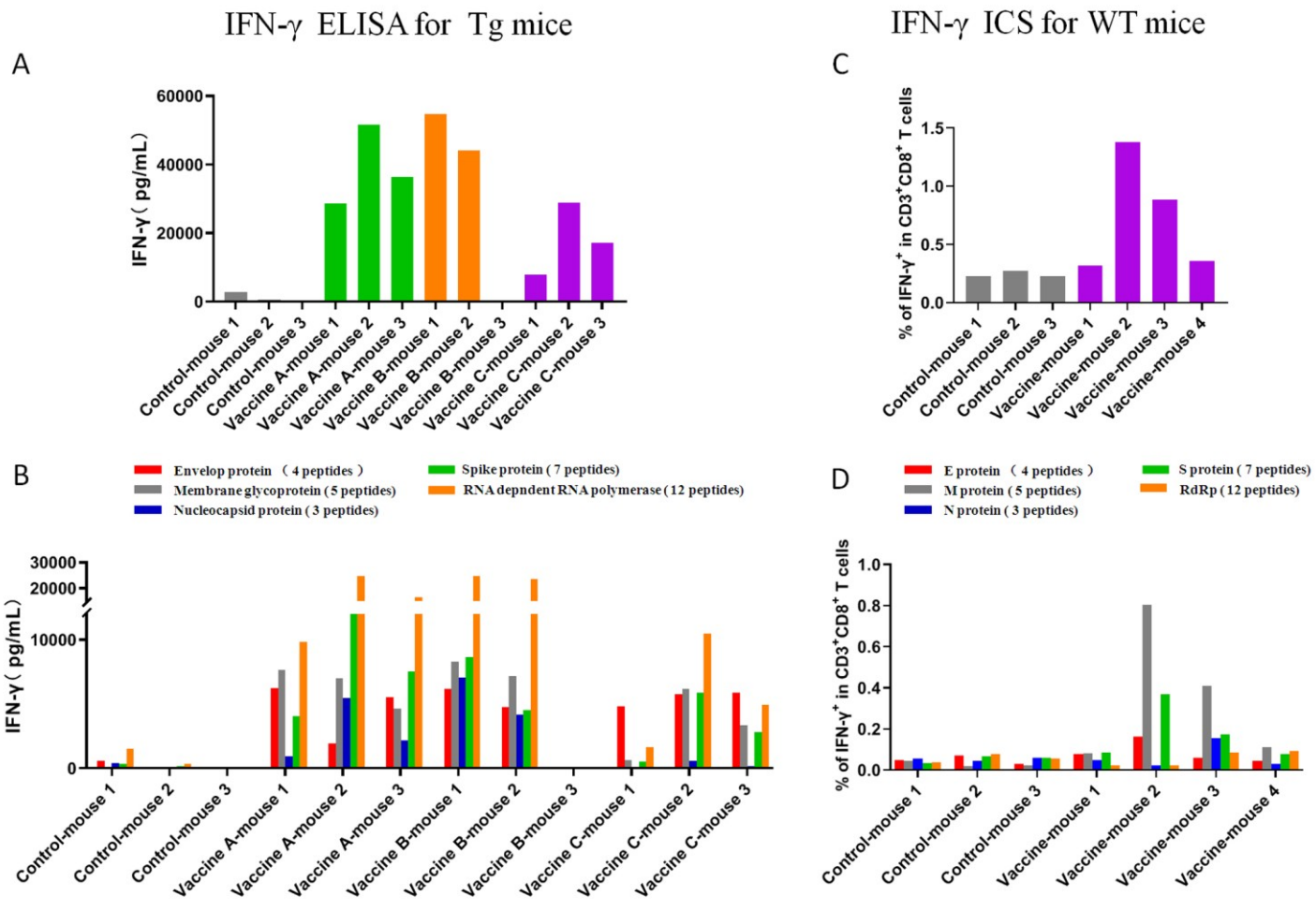

bioRxiv preprint doi: https://doi.org/10.1101/2021.04.01.438020; this version posted May 24, 2021. The copyright holder for this preprint (which was not certified by peer review) is the author/funder. All rights reserved. No reuse allowed without permission.
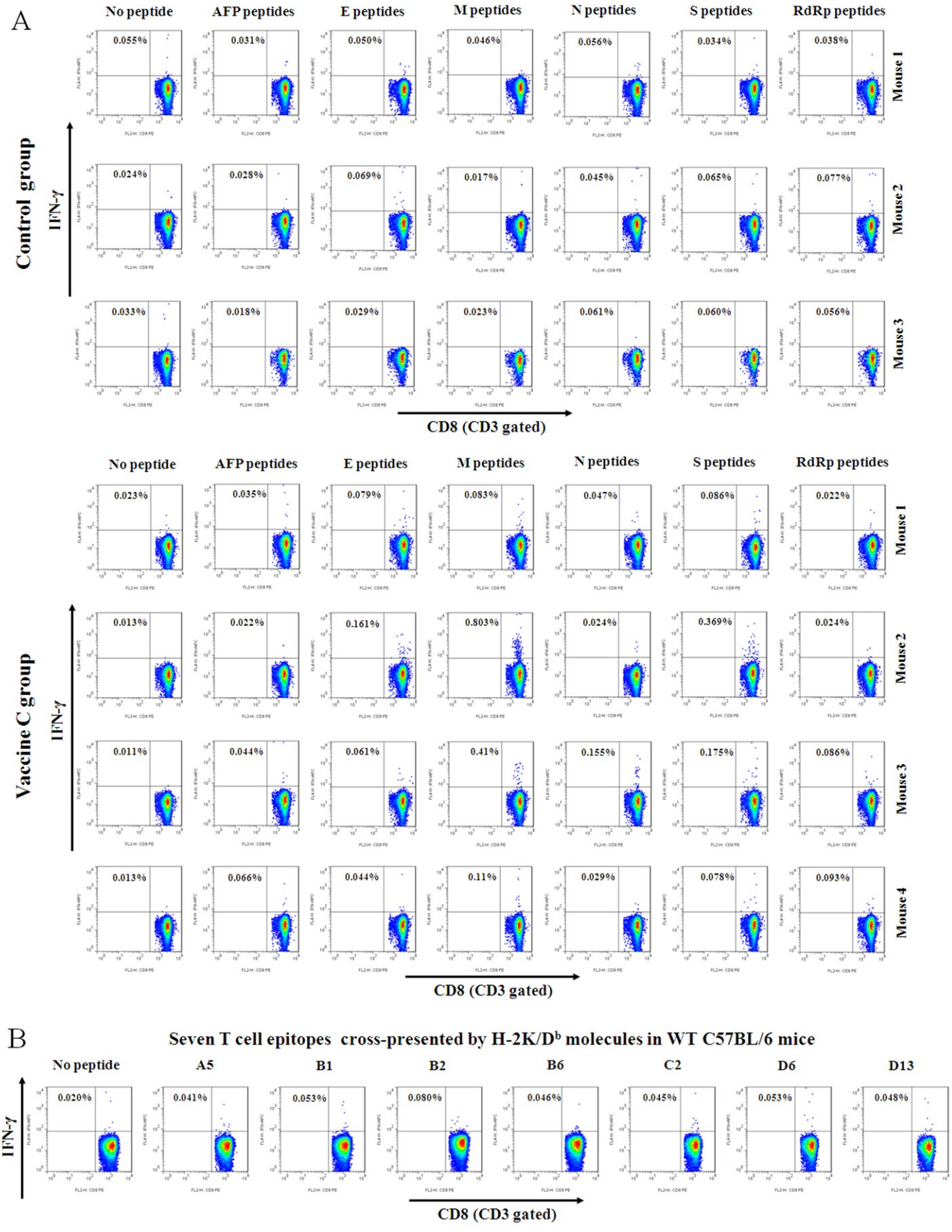
Figure 7: